SYNTHESIS AND CHARACTERIZATION OF TRANSPARENT CONDUCTIVE ZINC OXIDE THIN FILMS BY SOL-GEL SPIN COATING METHOD

David Winarski

A Thesis

Submitted to the Graduate College of Bowling Green
State University in partial fulfillment of
the requirements for the degree of

MASTER OF SCIENCE

August 2015

Committee:

Farida Selim, Advisor

Lewis P. Fulcher

Haowen Xi

ABSTRACT

Farida Selim, Advisor

Zinc oxide has been given much attention recently as it is promising for various semiconductor device applications. ZnO has a direct band gap of 3.3 eV, high exciton binding energy of 60 meV and can exist in various bulk powder and thin film forms for different applications. ZnO is naturally n-type with various structural defects, which sparks further investigation into the material properties. Although there are many potential applications for this ZnO, an overall lack of understand and control of intrinsic defects has proven difficult to obtain consistent, repeatable results.

This work studies both synthesis and characterization of zinc oxide in an effort to produce high quality transparent conductive oxides. The sol-gel spin coating method was used to obtain highly transparent ZnO thin films with high UV absorbance. This research develops a new more consistent method for synthesis of these thin films, providing insight for maintaining quality control for each step in the procedure. A sol-gel spin coating technique is optimized, yielding highly transparent polycrystalline ZnO thin films with tunable electrical properties.

Annealing treatment in hydrogen and zinc atmospheres is researched in an effort to increase electrical conductivity and better understand intrinsic properties of the material. These treatment have shown significant effects on the properties of ZnO.

Characterization of doped and undoped ZnO synthesized by the sol-gel spin coating method was carried out using scanning electron microscopy, UV-Visible range absorbance, X-ray diffraction, and the Hall Effect. Treatment in hydrogen shows an overall decrease in the number of crystal phases and visible absorbance while zinc seems to have the opposite effect.

The Hall Effect has shown that both annealing environments increase the n-type conductivity, yielding a ZnO thin film with a carrier concentration as high as 3.001×10^{21} cm^{-3}.

For the Winarski Family and Friends.

ACKNOWLEDGMENTS

I would like to thank Dr. Farida Selim for guiding my research and giving me the opportunity to learn various experimental techniques. This opportunity has offered exciting challenges to expand my knowledge and refine my technical skills.

I thank Team Selim and friends for their hard work and willingness to assist. Jianfeng Ji, Pooneh Saadatkia, Petr Stepanov, Sunil Thapa, Anthony Colosimo, Ben Hardy, Josh Mewhinney and the rest of BGSU Department of Physics and Astronomy have been a tremendous help in this research effort.

I thank Dr. Fulcher and Dr. Xi for agreeing to be committee members for my thesis defense.

Finally, I would like to thank my father, Jim, and mother, Lisa, and my siblings Nick, Christina, and Marie, for all of their support which has afforded me the opportunity to explore my interest in physics.

TABLE OF CONTENTS

Page

CHAPTER 1: INTRODUCTION TO ZINC OXIDE (ZnO) 1

1.1 Applications and Optical and Electronic Properties of ZnO 1

1.1.1 Blue Light Emitting Devices 1

1.1.2 Scintillators 2

1.1.3 Plasmonics 2

1.1.4 Gas Sensors 2

1.1.5 Transparent Conductive Oxide (TCO) Thin Films 3

1.2 Structural Defects of ZnO 3

1.2.1 Oxygen Vacancies 4

1.2.2 Zinc Vacancies 5

1.2.3 Zinc Interstitials 5

1.3 References 6

CHAPTER 2: SOL-GEL SYNTHESIS OF THIN FILM ZINC OXIDE BY SPIN COATING 10

2.1 Solution Preparation and Doping 10

2.2 Substrate Matching and Preparation 11

2.3 Thin Film Layering by Spin Coating 11

2.4 Heat Treatment of ZnO Thin Films 12

2.4.1 Drying 13

2.4.2 Furnace Annealing 13

2.5 Scope of Work 14

2.6 References 15

CHAPTER 3: EXPERIMENT AND RESULTS – SYNTHESIZING AND CHARACTERIZING ZINC OXIDE THIN FILMS 19

3.1 Preliminary Synthesis Effort 19

3.1.1 Sol-gel Spin Coating Synthesis of ZnO Thin Films 20

3.1.2 SEM Characterization 20

3.1.3 Conclusions 22

3.2 A Redeveloped Sol-gel Spin Coating Method 23

3.2.1 Substrate Preparation and Piranha Etching 24

3.2.2 Sol-gel Spin Coating Synthesis of 3% Al:ZnO Thin Films 25

3.2.3 SEM Characterization 27

3.2.4 Optical Characterization 36

3.2.5 Conclusions 41

3.3 An Optimized Sol-gel Spin Coating Method for ZnO Thin Films 42

3.3.1 Sol-gel Spin Coating Synthesis of ZnO Thin Films 44

3.3.2 SEM Characterization 45

3.3.3 Optical Characterization 49

3.3.4 XRD Characterization 50

3.3.5 Conclusions 53

3.4 Hydrogen Annealing Treatment and Effects on ZnO Thin Films 53

3.4.1 Optical Characterization and Positron Spectroscopy 53

3.4.2 XRD Characterization 58

3.4.3 Electrical Properties: Hall Effect and van der Pauw Methods 62

3.4.4 Conclusions 66

3.5 Zinc Annealing Treatment and Effects on ZnO Thin Films 66

3.5.1 Optical Characterization 67

3.5.2 XRD Characterization.....70

3.5.3 Electrical Properties: Hall Effect and van der Pauw Methods 75

3.5.4 Conclusions.....77

3.6 References.....77

CHAPTER 4: CONCLUSIONS AND FUTURE WORK.....78

APPENDIX A: DOPED AND UNDOPED ZnO THIN FILM SYNTHESIZED BY SOL GEL SPIN COATING.....81

APPENDIX B : STANDARD X-RAY PATTERNS FOR ZnO 85

APPENDIX C: STANDARD X-RAY PATTERNS FOR Al_2O_3 86

LIST OF TABLES

Table Page

3.1 Solution doping agents and percentage, substrate type and number of layers for 3% Al:ZnO thin films 26

3.2 XRD peak positions, separation and phase for undoped and 1% Al:ZnO thin films synthesized by sol-gel spin coating 52

3.3 XRD peak positions, separation and phase for 16 layer 1% Al:ZnO on AB etched quartz before and after hydrogen treatment 59

3.4 XRD peak positions, separation and phase for 16 layer 1% Ga:ZnO on AB etched quartz 61

3.5 Two-probe surface resistance measurements for 1%Al:ZnO, 1%Ga:ZnO after hydrogen treatment at 400ºC 62

3.6 Electric properties of 1%Ga:ZnO sample annealed in various hydrogen treatments at 400ºC measured by Hall and van der Pauw methods 65

3.7 XRD peak positions and error measurements for undoped ZnO thin films by sol- gel spin coating. One sample was post-annealed in a zinc atmosphere at 400ºC 72

3.8 XRD peak positions, separation and phase for 16 layer 1% Al:ZnO on AB etched quartz – post-annealed in H_2 at 400ºC – before and after treatment in zinc atmosphere 74

3.9 Two-probe surface resistance measurements for ZnO thin films after zinc treatment at 400ºC. Some samples were previously treated in hydrogen atmospheres at 400ºC 75

3.10 Electric properties of zinc oxide films after treatment in zinc atmospheres at 400ºC measured by Hall and van der Pauw methods 76

LISTS OF FIGURES

Figure Page

1.1 Wurzite structure of a ZnO single crystal 4

1.2 Zinc oxide lattice with oxygen vacancy and zinc interstitial defects....6

2.1 Diagram of the spin coating system....12

3.1 A schematic of a Scanning Electron Microscope 21

3.2 (a) SEM of 4 layers 1%Ga:ZnO on untreated sapphire 22

3.2 (b) SEM of 6 layers undoped ZnO on untreated sapphire 22

3.3 SEM of 6 layer 3% Al:ZnO thin films synthesized using aluminum acetate and layered on piranha BA quartz....27

3.4 SEM of 6 layer 3% Al:ZnO thin films synthesized using aluminum acetate and layered on piranha AB quartz....29

3.5 SEM of 6 layer 3% Al:ZnO thin films synthesized using aluminum chloride and layered on piranha AB quartz....31

3.6 SEM of a highly defective 6 layer 3% Al:ZnO thin films synthesized using aluminum chloride and layered on piranha BA quartz 33

3.7 (a) SEM of 12 layer 3%Al:ZnO from aluminum acetate precursor on piranha AB quartz....34

3.7 (b) SEM of 12 layer 3%Al:ZnO from aluminum chloride precursor on piranha AB quartz...34

3.8 (a) SEM of 12 layer 3%Al:ZnO from aluminum acetate precursor on piranha BA quartz....35

3.8 (b) SEM of 12 layer 3%Al:ZnO from chloride acetate precursor on piranha BA quartz....35

3.9 Diagram of Perkin Elmer Lambda 35 spectrometer 36

3.10 Absorbance spectrum for 6 layer 3% Al:ZnO thin films 37

3.11 (a) Electron-hole pair excitaton by photon absorbance 39

3.11 (b) Recombination of excited charge carriers.....39

3.12 Photoluminescence measurements for 3% Al:ZnO thin film samples 40

3.13 Summary of the optimized sol-gel spin coating method 43

3.14 SEM of 16 layer 1% Al:ZnO thin films synthesized by the optimized sol-gel spin coating technique on piranha AB quartz 45

3.15 SEM of 16 layer 3% Mn:ZnO thin films synthesized by the optimized sol-gel spin coating technique on piranha AB quartz 46

3.16 SEM of 16 layer 1% Co:ZnO thin films synthesized by the optimized sol-gel spin coating technique on piranha AB quartz 47

3.17 SEM Side-view of a cut 16 layer 1% Al:ZnO thin film sample to measure thickness.....48

3.18 Absorbance spectra of 12 layer undoped ZnO on AB etched quartz, 16 layer 1% Al:ZnO on AB etched quartz, and the quartz substrate.....49

3.19 XRD patterns for 12 layer undoped ZnO on AB etched quartz and 16 layer 1% Al:ZnO on AB etched quartz.....51

3.20 Absorbance spectra of 16 layer 1% Al:ZnO on AB etched quartz before and after hydrogen treatment at 400^{o}C for 1 hour.....54

3.21 Visible range absorbance for 1% Al:ZnO before and after H_2 treatment 56

3.22 Positron trapping for defect spectroscopy.....57

3.23 XRD patterns for 16 layer 1% Al:ZnO on AB etched quartz before and after hydrogen treatment 58

3.24 XRD patterns for 16 layer 1% Ga:ZnO on AB etched quartz before and after hydrogen treatment 60

3.25 Schematic of the Hall Effect of a semiconductor 63

3.26 Absorbance of undoped ZnO before and after annealing in Zn foil and N_2 atmosphere at 400^{o}C for 3 hours 67

3.27 Visible range absorbance of undoped ZnO before and after annealing in Zn foil and N_2 atmosphere at 400^{o}C for 1 hour 68

3.28 Visible range absorbance of 1%Al:ZnO – annealed in air at 400^{o}C for 1 hour, in H_2 at 400^{o}C for 1 hour – before and after anneal in zinc foil in N_2 at 400^{o}C for 1 hour.....69

3.29 XRD patterns for 12 layer Undoped ZnO on AB etched quartz before and after treatment in zinc atmosphere at 400^{o}C for 3 hours 71

3.30 XRD patterns for 16 layer 1% Al:ZnO on AB etched quartz – and post-annealed in H_2 at 400^{o}C – before and after treatment in zinc atmosphere at 400^{o}C for 1 and 3 hours.....73

CHAPTER 1: INTORDOCUTION TO ZINC OXIDE (ZnO)

This chapter discusses the basic properties and research applications of zinc oxide. It reviews current uses in research and devices – more specifically as a transparent conductive oxide – and discusses some of the optical, electrical, and structural properties of ZnO. It also reviews some synthesis and doping techniques and discusses intrinsic defects and the significant role they play on the optoelectronic properties of the material. Furthermore, this chapter examines heat treatment in various atmospheres and the effects it has on the material properties.

1.1 Applications and Optical and Electrical Properties of Zinc Oxide

Zinc oxide is a wide band gap semiconductor (3.3 eV) with promising room temperature applications due to its high exciton binding energy of 60 meV. ZnO exhibits high transparency and naturally n-type conductivity. The fundamental properties of this material have been investigated and has many potential applications in optoelectronics [1].

1.1.1 Blue Light Emitting Devices

Crystalline ZnO displays very high transparency in the visible light range. This coupled with its UV absorbance can make ZnO a useful material for optical devices. ZnO has shown effectiveness in light emitting devices and studying its luminescence can give us valuable information for enhancing material properties. ZnO displays photoluminescence in the blue and green-yellow regions. The blue region is related to exciton emission, which increases in intensity as the temperature decreases, and the green-yellow region is defect related and greatly depends on the synthesis method [2]. Research has shown that tuning structural characteristics of ZnO nanoparticles can greatly affect the optical properties. ZnO seems a more favorable prospect for blue LEDs than the current gallium nitride (GaN), as GaN has an exciton binding

energy of 26 meV. Unfortunately, lack of control over defects and doping makes it very difficult to achieve p-type ZnO [3].

1.1.2 Scintillators

Scintillators convert high energy ionizing radiation to photons for fast photodetectors. ZnO is a useful material for scintillation devices due to its sub-nanosecond decay time and intense light output. Its transparency and large number of bound excitons at room temperature allow for high intensity and ultrafast scintillation signals [4]. By varying dopants and their concentration in ZnO, the light output can significantly change [5]. Specifically, gallium has been used as a dopant – and nitrogen as a codopant – in ceramic ZnO to vary the intensities and ratios of band edge and intraband luminescence. Unfortunately, ceramic Ga:ZnO has not achieved optimal transparency in the visible range and the luminescence signal is quenched in comparison to undoped ZnO [6].

1.1.3 Plasmonics

Zinc oxide has also shown promising signs for applications in plasmonic devices. Silver and gold exhibit high loss in optical frequencies due to light dispersion. Therefore, it is difficult to tune these metals for application-specific properties. Plus, synthesis is incompatible with typical silicon technologies. ZnO semiconductors can help overcome these obstacles. Aluminum-doped ZnO/ZnO layered materials can replace conventional metals in plasmonics, as it exhibits low loss at optical frequencies and can be tuned for specific metal-like properties at infrared frequencies [8].

1.1.4 Gas Sensors

Zinc oxide can be used in many gas, chemical, and biological sensors due to its sensitive surface conductivity in different environments. Intrinsic donor oxygen vacancies can be filled,

resulting in a decrease in the number of charge carriers in the conduction band, and thus a decrease in surface conductivity. Conversely, there is an increase in surface conductivity in a hydrogen atmosphere. Hydrogen acts as a donor in ZnO and will passivate zinc vacancies, increasing the number of charge carriers in the conduction band [9]. The sensitive surface conductivity of Al:ZnO thin films has been tested for sensing freshness of food and presence of ethanol vapor [10-11].

1.1.5 Transparent Conductive Oxide (TCO) Thin Films

Doped zinc oxide thin films are a transparent conductive oxide (TCO) used as electrodes in thin film solar cells. The UV absorbance, high transparency between 400-1100 nm and electrical properties of ZnO are leading to increased attention of the material. ZnO exhibits carrier mobility similar to doped silicon semiconductors and provides cheaper, more accessible methods for synthesis. ZnO semiconductors can be synthesized using a variety of techniques, such as thermal diffusion, assisted-hydrothermal methods, magnetron sputtering, molecular beam epitaxy, along with many low temperature aqueous chemical growths [12-17]. Each of these processes has found success synthesizing doped and undoped zinc oxide, but an overall lack of doping control has led to many different properties of ZnO with the reasoning behind them up for debate.

1.2 Structural Defects of ZnO

Wide band gap materials, like ZnO, experience difficulty in doping control due to native defects in the material structure. Zinc oxide exists as a hexagonal wurzite structure in ambient conditions.

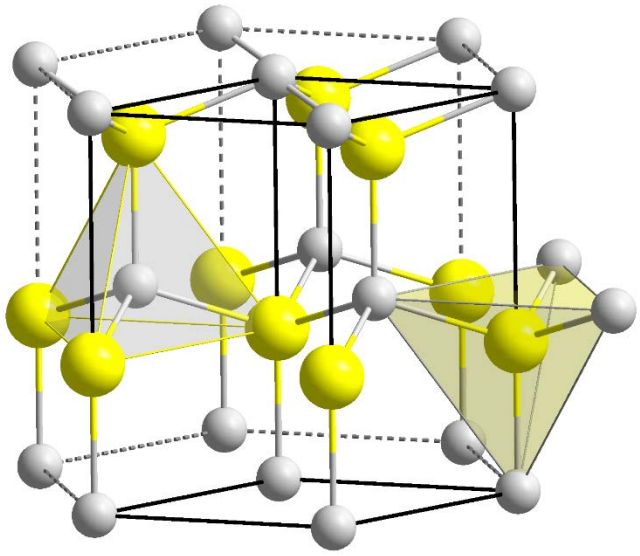

Figure 1.1 depicts the wurzite structure of a ZnO single crystal. This alignment yields four zinc (yellow) cations surrounding each oxygen (grey) anion [18].

In ZnO, native defects in the crystal lattice can influence the structure, affecting the optical and electrical properties and device quality, producing a naturally n-type material [1]. Furthermore, these donors in zinc oxide can compensate for the addition of acceptor dopants, preventing p-type conductivity. Structural defects can be dependent on the atmosphere in which the ZnO material is grown and a number of thermal treatment techniques post-synthesis. Characterizing the nature of defects in ZnO thin films will shed light on the material properties and possibilities for tuning.

1.2.1 Oxygen Vacancies

Oxygen vacancies are the most discussed defect in ZnO, as it was once believed to be one of the main sources for natural n-typing. But, density-functional theory calculates that oxygen vacancies are too deep to contribute to n-type conductivity [1]. Still, this defect is electrically and optically active, responsible for a green luminescence signal [19]. These deep donors can be

filled or manipulated in different annealing atmospheres, such as hydrogen, affecting the optical properties with reports of changing the color from red to transparent [20]. Therefore, annealing a ZnO thin film in an O_2 atmosphere will reduce the number of charge carriers, decreasing the photoluminescence signal [21].

1.2.2 Zinc Vacancies

Zinc vacancies can easily form as a deep acceptor in n-type ZnO. In oxygen rich atmospheres, a stronger photoluminescence signal is created at the 2.2eV peak, signifying a higher concentration of zinc vacancies. Hydrogen rich atmospheres also have an effect on these zinc vacancies. Due to hydrogen's donor-like nature, its incorporation into the structure will passivate the charge state of zinc vacancies. This in turn will increase the n-type conductivity. Evidence of this is shown because the green luminescence is quenched when oxygen-rich ZnO is doped with hydrogen [22].

1.2.3 Zinc Interstitials

Zinc interstitials bring two electrons above the conduction band minimum in order to stabilize its +2 charge state. These defects are not the source of n-type doping, as their formation energy is too low, but they can be source of p-type compensation [1]. Zinc interstitials are thought to be a deep donor because they have low ionization energy, but it is still unclear if it is related to sublattice defects or zinc-interstitial complex. Zinc interstitials have shown room temperature mobility, creating a complex with ambient nitrogen. This complex acts as a shallow donor and can increase the conductivity of ZnO [23].

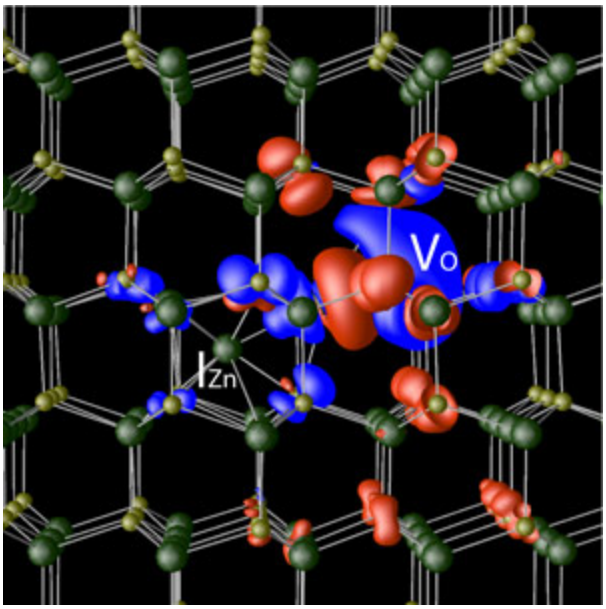

Figure 1.2 shows a zinc oxide lattice with oxygen vacancy, V_o, and zinc interstitial, I_{Zn}, defects. These defects cause a redistribution in positive (blue) and negative (red) charges, ultimately resulting in an increase in n-type conductivity [24].

1.3 References

[1] Janotti, Anderson, and Chris G. Van De Walle. "Fundamentals of Zinc Oxide as a Semiconductor." *Rep. Prog. Phys. Reports on Progress in Physics*72.12 (2009): 126501. Web.

[2] Grigorjeva, L., D. Millers, V. Pankratov, A. Kalinko, J. Grabis, and C. Monty. "Blue Luminescence in ZnO Single Crystals, Nanopowders, Ceramic." *J. Phys.: Conf. Ser. Journal of Physics: Conference Series* 93 (2007): 012036. Web.

[3] Zeng, Haibo, Guotao Duan, Yue Li, Shikuan Yang, Xiaoxia Xu, and Weiping Cai. "Blue Luminescence of ZnO Nanoparticles Based on Non-Equilibrium Processes: Defect Origins and Emission Controls."*Advanced Functional Materials Adv. Funct. Mater.* 20.4 (2010): 561-72. Web.

[4] Yanagida, Takayuki, Yutaka Fujimoto, Kohei Yamanoi, Masataka Kano, Akira Wakamiya, Shunsuke Kurosawa, and Nobuhiko Sarukura. "Optical and Scintillation Properties of Bulk ZnO Crystal." *Phys. Status Solidi C Physica Status Solidi (c)* 9.12 (2012): 2284-287. Web.

[5] Simpson, P.j., R. Tjossem, A.w. Hunt, K.g. Lynn, and V. Munné. "Superfast Timing Performance from ZnO Scintillators." *Nuclear Instruments and Methods in Physics Research Section A: Accelerators, Spectrometers, Detectors and Associated Equipment* 505.1-2 (2003): 82-84. Web.

[6] Gorokhova, E. I., G. V. Anan'eva, V. A. DemidFenko, P. A. Rodnyĭ, I. V. Khodyuk, and E. D. Bourret-Courchesne. "Optical, Luminescence, and Scintillation Properties of ZnO and ZnO:Ga Ceramics." *J. Opt. Technol. Journal of Optical Technology* 75.11 (2008): 741. Web.

[7] Boriskina, Svetlana V., Hadi Ghasemi, and Gang Chen. "Plasmonic Materials for Energy: From Physics to Applications." *Materials Today* 16.10 (2013): 375-86. Web.

[8] Naik, G. V., J. Liu, A. V. Kildishev, V. M. Shalaev, and A. Boltasseva. "Demonstration of Al:ZnO as a Plasmonic Component for Near-infrared Metamaterials." *Proceedings of the National Academy of Sciences* 109.23 (2012): 8834-838. Web.

[9] Zhang, Z., D. C. Look, R. Schifano, K. M. Johansen, B. G. Svensson, and L. J. Brillson. "Process Dependence of H Passivation and Doping in H-implanted ZnO." *Journal of Physics D: Applied Physics J. Phys. D: Appl. Phys.* 46.5 (2013): 055107. Web.

[10] Schmidt, Oliver, Peter Kiesel, Chris G. Van De Walle, Noble M. Johnson, Jeff Nause, and Gottfried H. Döhler. "Effects of an Electrically Conducting Layer at the Zinc Oxide Surface." *Japanese Journal of Applied Physics Jpn. J. Appl. Phys.* 44.10 (2005): 7271-274. Web.

[11] Chou, Shih Min, Lay Gaik Teoh, Wei Hao Lai, Yen Hsun Su, and Min Hsiung Hon. "ZnO:Al Thin Film Gas Sensor for Detection of Ethanol Vapor." *Sensors* 6.10 (2006): 1420-427. Web.

[12] Alivov, Ya. I., M. V. Chukichev, and V. A. Nikitenko. "Green Luminescence Band of Zinc Oxide Films Copper-doped by Thermal Diffusion." *Semiconductors* 38.1 (2004): 31-35. Web.

[13] López-Romero, S., and M. García-H. "Photoluminescence and Structural Properties of ZnO Nanorods Growth by Assisted-Hydrothermal Method." *WJCMP World Journal of Condensed Matter Physics* 03.03 (2013): 152-57. Web.

[14] Yang, Z., D. C. Look, and J. L. Liu. "Ga-related Photoluminescence Lines in Ga-doped ZnO Grown by Plasma-assisted Molecular-beam Epitaxy." *Applied Physics Letters Appl. Phys. Lett.* 94.7 (2009): 072101. Web.

[15] Le, Hong Quang, and Soo Jin Chua. "Gallium and Indium Co-doping of Epitaxial Zinc Oxide Thin Films Grown in Water at 90 °C." *Journal of Physics D: Applied Physics J. Phys. D: Appl. Phys.* 44.12 (2011): 125104. Web.

[16] Miyake, M., H. Fukui, T. Doi, and T. Hirato. "Preparation of Low-Resistivity Ga-Doped ZnO Epitaxial Films from Aqueous Solution Using Flow Reactor." *Journal of the Electrochemical Society* 161.14 (2014): n. pag. Web.

[17] Richardson, Jacob J., Gregory K. L. Goh, Hong Quang Le, Laura-Lynn Liew, Fred F. Lange, and Steven P. Denbaars. "Thermally Induced Pore Formation in Epitaxial ZnO Films Grown from Low Temperature Aqueous Solution." *Crystal Growth & Design* 11.8 (2011): 3558-563. Web.

[18] "Structure." *What Is Zinc Oxide?* N.p., n.d. Web. 10 June 2015. <http://whatiszincoxide.weebly.com/structure.html>.

[19] Wu, X. L., G. G. Siu, C. L. Fu, and H. C. Ong. "Photoluminescence and Cathodoluminescence Studies of Stoichiometric and Oxygen-deficient ZnO Films."*Applied Physics Letters Appl. Phys. Lett.* 78.16 (2001): 2285. Web.

[20] Selim, F. A., M. H. Weber, D. Solodovnikov, and K. G. Lynn. "Nature of Native Defects in ZnO." *Phys. Rev. Lett. Physical Review Letters* 99.8 (2007): n. pag. Web.

[21] Lv, Jinpeng, and Chundong Li. "Evidences of VO, VZn, and Oi Defects as the Green Luminescence Origins in ZnO." *Applied Physics Letters Appl. Phys. Lett.* 103.23 (2013): 232114. Web.

[22] Ton-That, C., L. Weston, and M. R. Phillips. "Characteristics of Point Defects in the Green Luminescence from Zn- and O-rich ZnO." *Physical Review B Phys. Rev. B* 86.11 (2012): n. pag. Web.

[23] Look, D. C., G. C. Farlow, Pakpoom Reunchan, Sukit Limpijumnong, S. B. Zhang, and K. Nordlund. "Evidence for Native-Defect Donors in N -Type ZnO." *Phys. Rev. Lett. Physical Review Letters* 95.22 (2005): n. pag. Web.

[24] *Nature.com*. Nature Publishing Group, n.d. Web. 10 June 2015. <http://www.nature.com/am/journal/2009/200906/full/am2009160a.html>.

CHAPTER 2: SOL-GEL SYNTHESIS OF THIN FILM ZINC OXIDE BY SPIN COATING

Thin film layers allow us access to nanoscale properties of many optoelectronic materials. Being able to synthesize thin film materials gives us a greater understanding of their intrinsic properties and a greater control of extrinsic defects. The "sol-gel" method is a non-toxic low temperature, low cost method which allows for simple addition of extrinsic defects and treatment of samples to optimize material properties. ZnO, among many other materials, has been synthesized using solution-based, dip coating and spin coating methods, giving the user layer-by-layer control of the material. The spin coating technique provides consistent layering for better control of film uniformity and thickness [26-27]. This chapter helps us understand how the sol-gel spin coating spin coating technique affects the properties of ZnO and provide us valuable information for application-specific optoelectronic devices. It also introduces the main goal and outlines the procedure of this research effort.

2.1 Solution Preparation and Doping

In order to obtain ZnO thin films, a homogeneous, transparent precursor solution must be made first. ZnO precursor solutions can be obtained by mixing zinc acetate dihydrate into a number of different solvents, such as isopropanol, methanol, ethanol, 2-methoxyehtnaol and adding a stabilizer, such as ethanolamine or diethanolamine. This mixture is heated and stirred until it homogenous and transparent, when it can be used for thin film synthesis. The mixture in the precursor solution can greatly affect the properties of the ZnO thin film. For example, the ZnO solution can be doped with other metals, such as gallium, copper, cobalt, and aluminum to tune the optoelectronic and ferromagnetic properties [28-31].

There has been much success doping ZnO thin films with group III elements, such as aluminum and gallium, due to their ionic radius. The Al^{3+} ionic radius is small than Zn^{2+} and can

easily replace Zn^{2+} in the lattice, but will lead to more lattice deformations. Ga^{3+} has an ionic radius very similar to Zn^{2+}, so it can replace Zn^{2+} but will produce far less lattice deformations than Al^{3+} [32]. Many studies have successfully synthesized polycrystalline Al- and Ga-doped ZnO thin films with very high transparency and promising electrical properties. These group III elements act as shallow donors when doping ZnO to increase overall conductivity for use as a transparent conductor [31, 33-34].

2.2 Substrate Matching and preparation

To investigate the properties of ZnO thin films, specific substrates must be considered. For TCOs, the thin film must be grown on an insulating substrate with high transparency in UV and visible ranges to differentiate the optical and electrical properties. Quartz and sapphire substrates have these qualities and are chemically active with surrounding atmospheres. Therefore they can be treated by cleaning and etching techniques to eliminate impurities and induce surface interactions. When oxides are placed in an acidic solution, the surface yields a net positive charge. Additionally, as an oxide bathes in a basic solution, the surface will have a net negative charge [35]. Substrates are etched in acidic, basic, and piranha solutions to induce a change in surface roughness for each cleaning technique [36]. For hydrofluoric acid etched silicon dioxide, the surface charge is shown to be pH dependent [37-38].

2.3 Thin Film Layering by Spin Coating

The spin coating technique has the ability to achieve large scale uniform thin film layering at precise thicknesses using basic chemistry and technology.

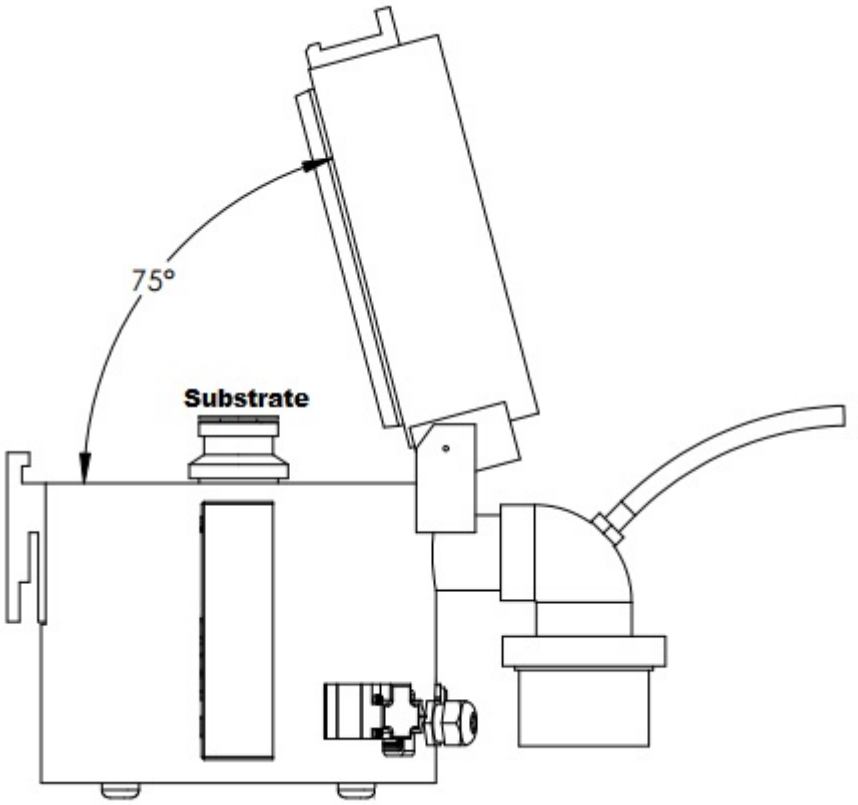

Figure 2.1 is a diagram of the spin coating system. A substrate is held to a platform by vacuum suction. The lid is closed, the platform for begins spinning and the solution is dispensed by syringe through a hole on top [39].

A ZnO precursor solution is dispensed and will cover the substrate in gel-like ZnO. After evaporating the solvent, the subsequent ZnO thin films exhibit a highly transparent polycrystalline structure [40]. Furthermore, ZnO thin film thickness and roughness are dependent on the spin coating process, especially the final spin rate and solvent evaporation stages [41-42]. Following the spin coating onto substrates, ZnO thin films can be thermally treated in different atmospheres to tune structural and electrical properties.

2.4 Thermal Treatment of Zinc Oxide Thin films

Thermal treatment of ZnO thin films can happen at various stages of the sol-gel spin coating process. Non-reactive E-beam evaporated thin films yield high transparency before and

after heat treatment. As annealing temperature increase, crystallinity worsens and resistivity improves [43]. Chemical spray method ZnO thin films display a shift in the band gap with treatment temperatures [44]. Understanding how to control heat treatment is important in helping tune the material properties of ZnO thin films, leading to promising device applications. The sol-gel spin coating method can be repeated for a desired number of layers. Usually, between each layer, the ZnO thin film is subject to drying.

2.4.1 Heat drying

Thin film drying typically takes place in an oven or on a hot plate ranging from room temperature to 300 degrees C. For temperatures greater than 100 degrees C, a large percentage of the thin film weight is lost, as the solvent quickly evaporates [45]. After achieving a desired thickness, the ZnO thin film is subject to other forms of thermal treatment at higher temperatures in more controlled atmospheres.

2.4.2 Furnace Annealing

Annealing in a furnace has significant effects on structure and surface morphology of ZnO thin films. ZnO thin films have been annealed in a temperature range between 300-500^{o}C to show an increase in c-axis (002) orientation and grain size with an increase in temperature [45]. These films still exhibit high transparency with tunable properties for optoelectronic use. Sol-gel synthesis and thermal treatment of ZnO thin films consistently produce structured, transparent thin films. These films are also subject to different atmospheres post-synthesis which can help tune the electrical properties.

Hydrogen in semiconductors is electrically active and acts solely as a donor in zinc oxide. Also, hydrogen is known to passivate defects in ZnO and on quartz interfaces. By heat treating zinc oxide in a hydrogen atmosphere, the electrical properties are greatly affected. This extra

addition of hydrogen creates interstitial donors and can passivate zinc vacancies which is known to increase the overall conductivity of zinc oxide [46].

Studies have shown that annealing Al- and Ga-doped ZnO thin films in air and then H_2 will yield highly transparent, lowly resistive thin films. When spin coating ZnO thin films with 1% aluminum precursor, the minimal resistivity achieved was 4.06×10^{-3} Ω cm with a carrier concentration as high as 5.52×10^{19} cm^{-3} after post-annealing in air [46]. ZnO thin films doped with 2% gallium yields highly transparent thin films with resistivity as low as 3.3×10^{-3} Ω cm after post-annealing in H_2 atmosphere [47].

2.5 Scope of Work

It is clear that zinc oxide is promising for a wide variety of applications for its structural, optical, and electrical properties. Transparent ZnO has been synthesized using many different techniques allowing us to better understand the material properties and the effects of doping and film treatment. ZnO's natural n-type conductivity is apparent, but it is not fully understood. Oxygen vacancies and zinc interstitials are the possible candidates for this debate, but must be studied further. The sol-gel technique affords a simple and inexpensive way to synthesize transparent doped and undoped ZnO thin films and treat these films under a heated atmosphere to manipulate and study the film properties.

The main goal of this work is to develop a sol-gel spin coating technique that yields high quality transparent doped and undoped ZnO thin films and use various atmospheric heat treatments to optimize electrical properties. The sol-gel spin coating technique is used to obtain highly transparent, polycrystalline Al- and Ga-doped and undoped ZnO thin films. These films are then subject to heat treatment in H_2 and Zn atmospheres in an effort to increase the n-type

conductivity. Overall, we want a ZnO thin film suitable for use as a transparent conductive oxide.

Chapter 3 details the sol-gel spin coating technique for uniform, highly transparent polycrystalline doped and undoped ZnO thin films. Furthermore, it discusses characterization techniques and provides experimental results and analysis of transparent conductive zinc oxide thin films synthesized by the sol-gel spin coating technique. Finally, Chapter 4 summarizes these results to determine the effectiveness of the sol-gel method for synthesis of transparent ZnO thin films. It also discusses the implications of the results for optimizing the material properties.

2.6 References

[26] Cruz, M. R. Alfaro, G. Ortega Zarzoza, G. A. Martinez Castanon, and J. R. Martinez. “Thin films from different materials obtained by the Sol-Gel method: study of the morphology through Atomic Force Microscopy (AFM),” *Current Microscopy Contributions to Advances in Science and Technology (A. Méndez-Vilas, Ed.)* (2012): 1370-1376. Web.

[27] Kamaruddin, Sharul Ashikin, Kah-Yoong Chan, Ho-Kwang Yow, Mohd Zainizan Sahdan, Hashim Saim, and Dietmar Knipp. "Zinc Oxide Films Prepared by Sol–gel Spin Coating Technique." *Appl. Phys. A Applied Physics A* 104.1 (2010): 263-68. Web.

[28] Guo, Dongyun, Kuninori Sato, Shingo Hibino, Tetsuya Takeuchi, Hisami Bessho, and Kazumi Kato. "Low-temperature Preparation of Transparent Conductive Al-doped ZnO Thin Films by a Novel Sol–gel Method." *Journal of Materials Science J Mater Sci*49.14 (2014): 4722-734. Web.

[29] Wu, S. Z., H. L. Yang, X. G. Xu, J. Miao, and Y. Jiang. "Ferromagnetism Studies of Cu-doped and (Cu, Al) Co-doped ZnO Thin Films." *J. Phys.: Conf. Ser. Journal of Physics: Conference Series* 263 (2011): 012022. Web.

[30] Foo, K.l., M. Kashif, U. Hashim, and M.e. Ali. "Fabrication and Characterization of ZnO Thin Films by Sol-Gel Spin Coating Method for the Determination of Phosphate Buffer Saline Concentration." *Current Nanoscience CNANO* 9.2 (2013): 288-92. Web.

[31] Znaidi, Lamia, Tahar Touam, Dominique Vrel, Nacer Souded, Sana Yahia, Ovidiu Brinza, Alexis Fischer, and Azzedine Boudrioua. "AZO Thin Films by Sol-Gel Process for Integrated Optics." *Coatings* 3.3 (2013): 126-39. Web.

[32] Liu, Yanli, Yufang Li, and Haibo Zeng. "ZnO-Based Transparent Conductive Thin Films: Doping, Performance, and Processing." *Journal of Nanomaterials* 2013 (2013): 1-9. Web.

[33] Wang, Fang-Hsing, Ching-Tien Chou, Tsung-Kuei Kang and Chia-Cheng Huang. “Structural, electrical, and optical properties of carbon nanotube-incorporated Al-doped zinc oxide thin films prepared by sol-gel method.” *Journal of Ceramic Processing Research* (2013): 149-152. Web

[34] Shrestha, Shankar Prasad, Rishi Ghimire, Jeevan Jyoti Nakarmi, Young-Sun Kim, Sabita Shrestha, Chong-Yun Park, and Jin-Hyo Boo. “Properties of ZnO:Al Films Prepared by Spin Coating of Aged Precursor Solution.” *112 Bull. Korean Chem. Soc.* (2010). Web.

[35] Raghavan, Srini. “Wet Etching and Cleaning: Surface Considerations and Process Issues.” 1999. *Microsoft Powerpoint* file.

[36] Kirby, Kevin W., Karthik Shanmugasundaram, V. Bojan, and J. Ruzyllo. "Interactions of Sapphire Surfaces with Standard Cleaning Solutions." *ECS Transactions* (2007): n. pag. Web.

[37] Knotter, D. Martin. "Etching Mechanism of Vitreous Silicon Dioxide in HF-Based Solutions." *J. Am. Chem. Soc. Journal of the American Chemical Society* 122.18 (2000): 4345-351. Web.

[38] Vos, Wiebe M. De, Beatrice Cattoz, Michael P. Avery, Terence Cosgrove, and Stuart W. Prescott. "Adsorption and Surfactant-Mediated Desorption of Poly(vinylpyrrolidone) on Plasma- and Piranha-Cleaned Silica Surfaces." *Langmuir* 30.28 (2014): 8425-431. Web.

[39] "Product Literature." *Spin Coater Literature / Brochures*. N.p., n.d. Web. 10 June 2015. <http://www.laurell.com/literature/WS-650-23B.pdf>.

[40] Ilican, S., Y. Caglar, M. Caglar. "Preparation and characterization of ZnO thin films deposited by sol-gel spin coating method." *Journal of Optoelectronics and Advanced Materials* (2008): 2578 – 2583. Web.

[41] W., Shivaraj B., H. N. Narasimha Murthy, M. Krishna, and S. C. Sharma. "Investigation of Influence of Spin Coating Parameters on the Morphology of ZnO Thin Films by Taguchi Method." *Int. J. Thin Film Sci. Tec. International Journal of Thin Films Science and Technology* 2.2 (2013): 143-54. Web.

[42] Sahu, Niranjan, B. Parija, and S. Panigrahi. "Fundamental Understanding and Modeling of Spin Coating Process: A Review." *Indian Journal of Physics Indian J Phys* 83.4 (2009): 493-502. Web.

[43] Golshahi, S., S. M. Rozati, T. Ghasempoor. “Annealing Treatment of ZnO Thin Films Prepared by Non-reactive E-beam Evaporation Technique.” *Digest Journal of Nanomaterials and Biostructures* (2011): 445 – 450. Web.

[44] Nasser, Ghazi Y., “Effect of Heat Treament on the Optical Properties of ZnO Thin Films Prepared by Spray Method.” *Iraqi Journal of Applied Physics* (2013). Web.

[45] Raoufi, Davood, and Taha Raoufi. "The Effect of Heat Treatment on the Physical Properties of Sol–gel Derived ZnO Thin Films." *Applied Surface Science* 255.11 (2009): 5812-817. Web.

[46] Salam, Shahzad, Mohammad Islam, and Aftab Akram. "Sol–gel Synthesis of Intrinsic and Aluminum-doped Zinc Oxide Thin Films as Transparent Conducting Oxides for Thin Film Solar Cells." *Thin Solid Films* 529 (2013): 242-47. Web.

[47] Nayak, Pradipta K., Jinwoo Kim, Seungjun Chung, Jaewook Jeong, Changhee Lee, and Yongtaek Hong. "Spin-coated Ga-doped ZnO Transparent Conducting Thin Films for Organic Light-emitting Diodes." *Journal of Physics D: Applied Physics J. Phys. D: Appl. Phys.* 42.13 (2009): 139801. Web.

CHAPTER 3: EXPERIMENT AND RESULTS – SYNTHESIZING AND CHARACTERIZING ZINC OXIDE THIN FILMS

This chapter describe the sol-gel spin coating technique used to make transparent conductive zinc oxide thin films. It explains different doping procedures, substrate preparations and spin coating techniques tried in an effort achieve high quality thin films. After each research effort, the sol-gel technique was redeveloped based on the characterization of the ZnO thin films synthesized. For a list of all doped and undoped ZnO thin films synthesized by sol-gel spin coating refer to Appendix A.

Chapter 3 also discusses the post-synthesis annealing techniques used to tune the material properties for improved structure and conductivity, while maintaining transparency. In addition, the properties of ZnO thin films are characterized by scanning electron microscopy, visible range absorbance, photoluminescence, X-ray diffraction, and the Hall Effect.

3.1 Preliminary Synthesis Effort

The sol-gel spin coating technique uses a precursor solution that is prepared using 2-methoxyethanol and ethanolamine (MEA), as a solvent and stabilizer respectively. High purity zinc acetate salt is easily dissolved into the solvent to make a 0.75 M transparent homogeneous zinc oxide solution at a 1:1 molar ratio with MEA. This precursor can be doped with various group III metals, specifically aluminum and gallium to add donor elements at zinc lattice sites. Aluminum and gallium salts can replace some zinc acetate to dope the precursor solution with donor ions while having little to no effect on the visible transparency of the solution. It is expected that lower concentrations of these doping agents (0-3% w/w) are most suitable for transparent conductive zinc oxide thin films.

3.1.1 Sol-gel Spin Coating Synthesis of ZnO Thin Films

Undoped ZnO and 1% Ga:ZnO precursor solutions are heated to 60^{o}C and stirred for 2 hours to obtain a transparent homogeneous solution. The solution is then cooled to room temperature to prepare it for the spin coating. Over time the solution will become more viscous, affecting the resultant thin film properties. Furthermore, the appropriate substrate selection is imperative for both synthesizing and analyzing zinc oxide thin films. Sapphire is used because it is insulating and highly transparent in the visible range.

At first, 1% Ga:ZnO and undoped ZnO thin films were spin coated onto untreated 10mm x 10mm sapphire substrates using an automatic dispenser. The substrate accelerates to 500 rpm and the solution is dispensed automatically onto the surface in a continuous stream. After a few seconds, the substrate was accelerated to 3000 rpm to evenly coat the substrate with zinc oxide. These films were placed in an oven at 80^{o}C for 10 minutes to evaporate the remaining solvent. The film was cooled and the layering process was repeated for 4-6 layers before the films were finally placed in a furnace in ambient air at 600^{o}C for 1 hour. The film quality can be investigated using a scanning electron microscope (SEM).

3.1.2 SEM Characterization

To study the effectiveness of these films, we can look at the surface using SEM to focus an electron beam on the sample. These electrons will interact with the sample, giving off detectable signals to give a nanometer scale image of the surface. Many lenses and detectors are involved to control the beam and account for backscattered electrons and other electromagnetic radiation.

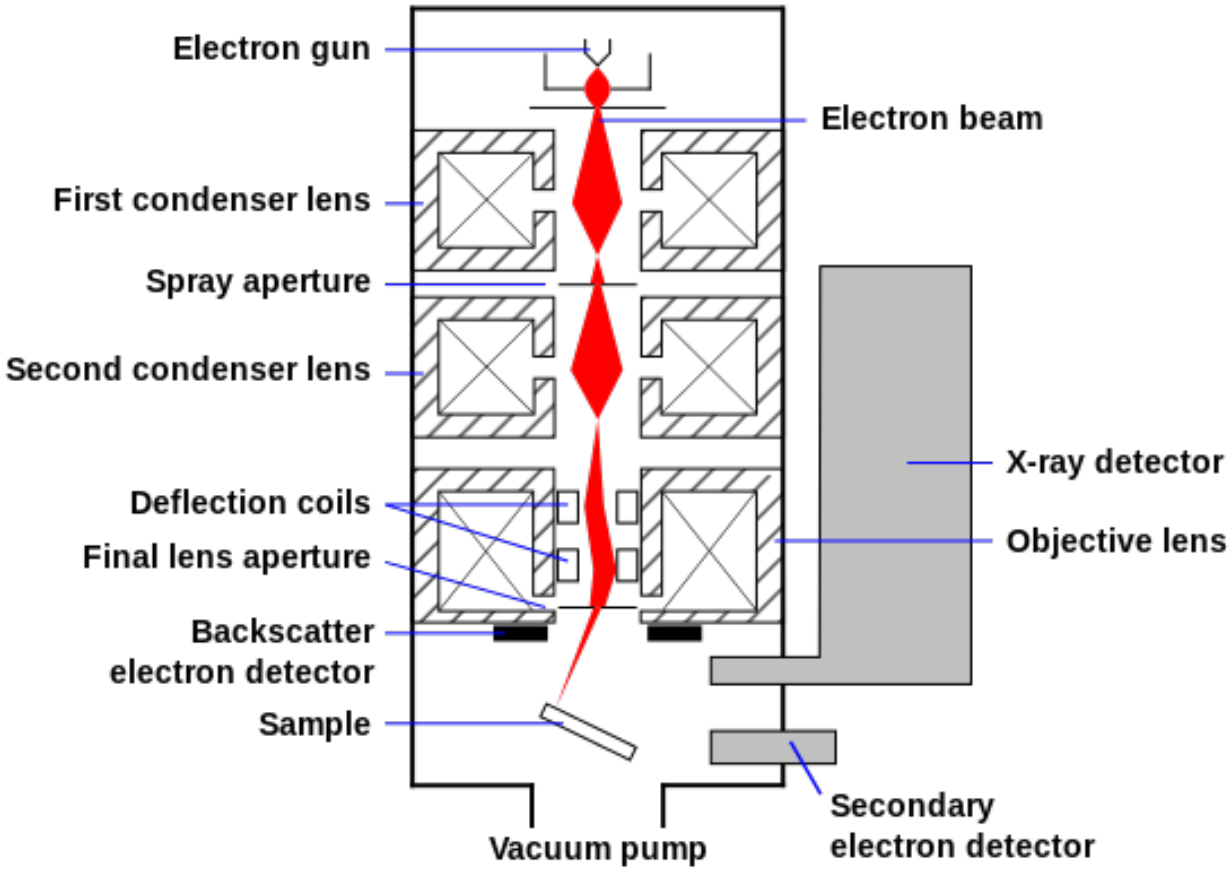

Figure 3.1 is a schematic of a Scanning Electron Microscope, showing the configuration of optics and detectors involved in sample measurements [48].

Using SEM analysis, it is clear to see that the zinc oxide thin films spin coated on 10x10 mm sapphire are very low quality as seen in Figure 2.

(a) 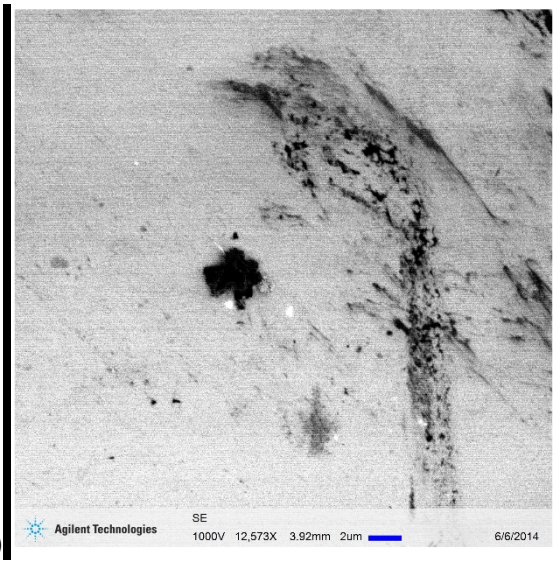

(b) 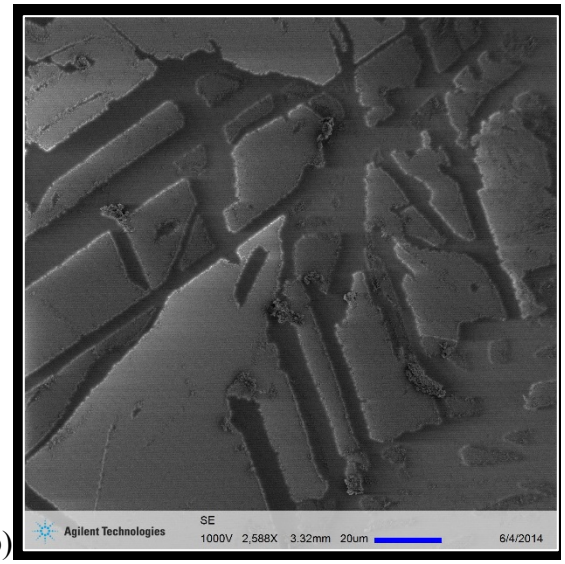

Figure 3.2 (a) is the surface of 4 layers 1%Ga:ZnO on untreated sapphire (b) and 6 layers undoped ZnO on untreated sapphire. These films are discontinuous, non-uniform layering with a lack of substrate coverage preventing any conductivity.

Although there is zinc oxide on the substrate, it is clear these thin films are useless, possibly due to overly viscous solutions, incompatible substrates, environmental impurities and an undeveloped spin coating technique which lacks control and consistency.

3.1.3 Conclusions

The first obstacle can be easily accounted for, by monitoring the solution and using it soon after synthesis so it does not become overly viscous. To overcome the some of the other issues, we considered using larger transparent substrates which can be pretreated in a series of piranha solutions to remove crude impurities and to control the surface reactivity and charge. It is believed the larger substrates will allow for more uniform spreading because of reduced edge effects. Also, an etching pretreatment will increase compatibility and rid the surface of

impurities. Solution and substrate compatibility is very important to successfully make layers of zinc oxide.

Along with the solution and substrate preparations, the layering process has many different variables that must be controlled to achieve high quality thin films. For instance, too much solution can result in chemical wrap around and excess waste, degrading the spin coater and requiring cleaning and maintenance. For this, a small manual syringe can be used to dispense the zinc oxide solution drop-by-drop, to fully coat the substrate and minimize excess solution.

Although discontinuities in the thin films arise for many reasons, it is believed that increasing the number of coatings and the amount of solution will help fill in gaps and defects from the previous layer and help achieve overall uniformity and coverage. Furthermore, the boiling point of 2-methoxyethanol is 125^{o}C. As our first attempt dried the films at 80^{o}C, there is a possibility that the solvent did not completely evaporate, preventing structured ZnO from forming.

Overall, our first attempt yielded substrates covered in inconsistent ZnO layers with far too many defects. Therefore, a sol-gel technique must be redeveloped to obtain high quality thin films for optoelectronic use.

3.2 A Redeveloped Sol-gel Spin Coating Technique

As discovered from our first attempts, there are many complications that must be overcome to successfully synthesize high quality doped and undoped ZnO thin films using the sol-gel spin coating method. It is believed these complications can be minimized by preparing the substrates in a piranha etch, monitoring the precursor solution, and controlling layering technique.

3.2.1 Substrate Preparation by Piranha Etching

Quartz substrates, 1 inch in diameter, have high visible range transparency and a larger area to achieve more uniform coverage. These larger substrates are treated in a series of piranha solutions in an effort to achieve a higher compatibility than the previously used sapphire.

Piranha solutions are mixture of hydrogen peroxide with a strong acid or a strong base. When a material is placed in this environment the solution react with crude impurities and hydroxyl and oxygen defects on the surface, which can greatly affect its interactions with other environments. The piranha AB etching procedure is as follows:

1. Place quartz substrate into $80^{O}C$ 3:1 H_2SO_4:H_2O_2 piranha acid solution – 100 mL – for 15 minutes.
2. Rinse thoroughly with deionized water.
3. Place quartz substrate into $80^{O}C$ 3:1 NH_4OH:H_2O_2 piranha base solution – 100 mL – for 15 minutes.
4. Rinse thoroughly in deionized water.
5. Dry in oven.

During step 1, the strong acid reacts with the negatively charges surface ions to induce a net positive charge on the surface of the substrate. Step 3 will have the opposite effect and leave a net negative surface charge. The order of the piranha acid and base solutions can be switched (piranha BA etch) to leave an overall net positive surface charge. The final etch solution determines the subsequent surface charge. Once the substrate is dried, it is cooled to room temperature and ready for the spin coating process.

3.2.2 Sol-gel synthesis of 3% Al:ZnO thin films

The sol-gel spin coating technique was redeveloped for synthesis of Al:ZnO thin films. Aluminum acetate and aluminum chloride were used as doping agents to synthesize 3% Al:ZnO precursor solutions. In most cases, aluminum acetate yielded cloudy solutions, as it does not completely dissociate in 2-methoxyethanol at 60^{o}C for 2 hours. On the other hand, aluminum chloride yielded more homogeneous, transparent solutions. These solutions were dispensed drop-by-drop with a manual syringe onto spinning quartz substrates prepared in piranha etches AB and BA. This more controlled technique with pretreated substrates can improve layering and consistency to decrease the number of defects in the thin films. 6 or 12 layers were deposited to ensure coverage and each layer was placed on a hot plate at 210^{o}C to ensure maximum solvent evaporation. After layering, these films were annealed in ambient air to enhance structural properties of the thin film. The following table summarizes the first thin films synthesized using the redeveloped sol-gel technique.

Table 3.1 Solution doping agents and percentage, substrate type and number of layers for 3% Al:ZnO thin films.

Dopant	Doping %	Quartz Etch	# of Layers	Comments
$Al(CH_3COO)\cdot OH$	3.0%	AB	6	Cloudy Solution
$Al(CH_3COO)\cdot OH$	3.0%	BA	6	Cloudy Solution
$AlCl_3\cdot xH_2O$	3.0%	AB	6	Transparent Solution
$AlCl_3\cdot xH_2O$	3.0%	BA	6	Transparent Solution
$Al(CH_3COO)\cdot OH$	3.0%	AB	12	Cloudy Solution
$Al(CH_3COO)\cdot OH$	3.0%	BA	12	Cloudy Solution
$AlCl_3\cdot xH_2O$	3.0%	AB	12	Transparent Solution
$AlCl_3\cdot xH_2O$	3.0%	BA	12	Transparent Solution

During the drying stage, a visible color change was observed and the thin films also turned cloudy and rough. The rapid temperature change may cause cracking and other discontinuities in the structure of the film. Furthermore, the thin films were not at room temperature during spin coating. This caused some solvent to evaporate while the solution was spreading across the substrate, greatly affecting the layering. At least 5 minutes is needed to cool to the substrates to room temperature in between each layer.

The annealing treatment will remove any remaining impurities and enhance the structure by filling vacancies. In our initial effort, our zinc oxide thin films were annealed at 600^{o}C, but research suggests annealing between 300-500^{o}C for optimal conductivity. Therefore, ZnO thin films are annealed after synthesis in ambient air at 400^{o}C for 1 hour. Once this process is complete the 3% Al:ZnO thin films are characterized using SEM.

3.2.3 SEM Characterization of 3% Al:ZnO Thin Films

Using SEM analysis, it is clear to see that the Al:ZnO thin films spin coated on pretreated 1 inch diameter quartz substrates are of higher quality than achieved in Figure 3.2.

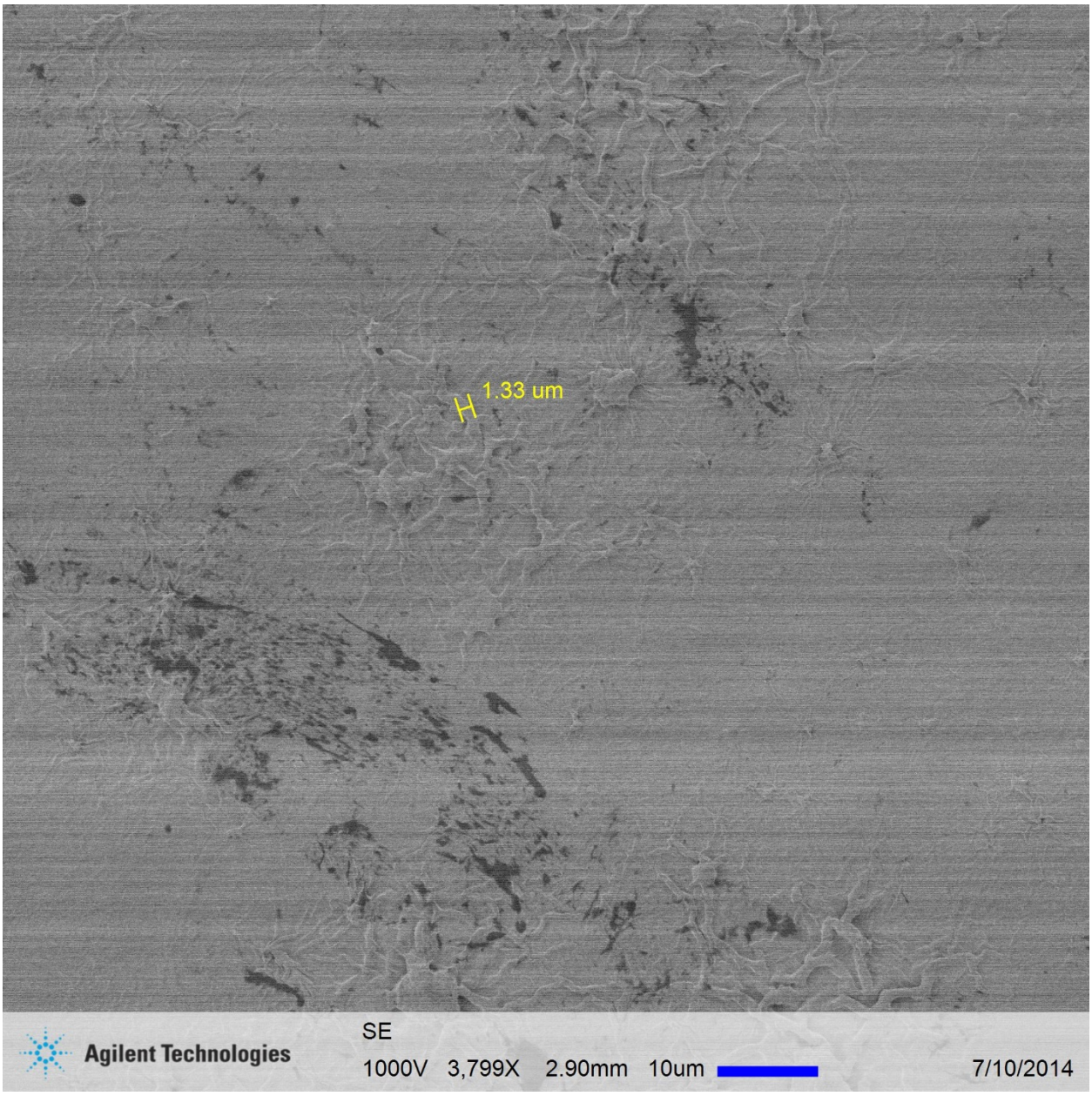

Figure 3.3 is the surface of 6 layer 3% Al:ZnO thin films synthesized using aluminum acetate and layered on piranha BA quartz. The thin film is non-uniform and has many defected areas not completely covering the substrate.

Although this film has many defects and is low quality, there are some clustered areas of structured zinc oxide growth. The inconsistent coverage and non-uniformity may be because the precursor solution was not homogeneous. Also, the lack of coverage could very be due to the minimal number of layers. Another 6 layer 3% Al:ZnO thin film on piranha AB quartz was synthesized using aluminum acetate was observed with SEM to reveal good overall coverage and uniformity.

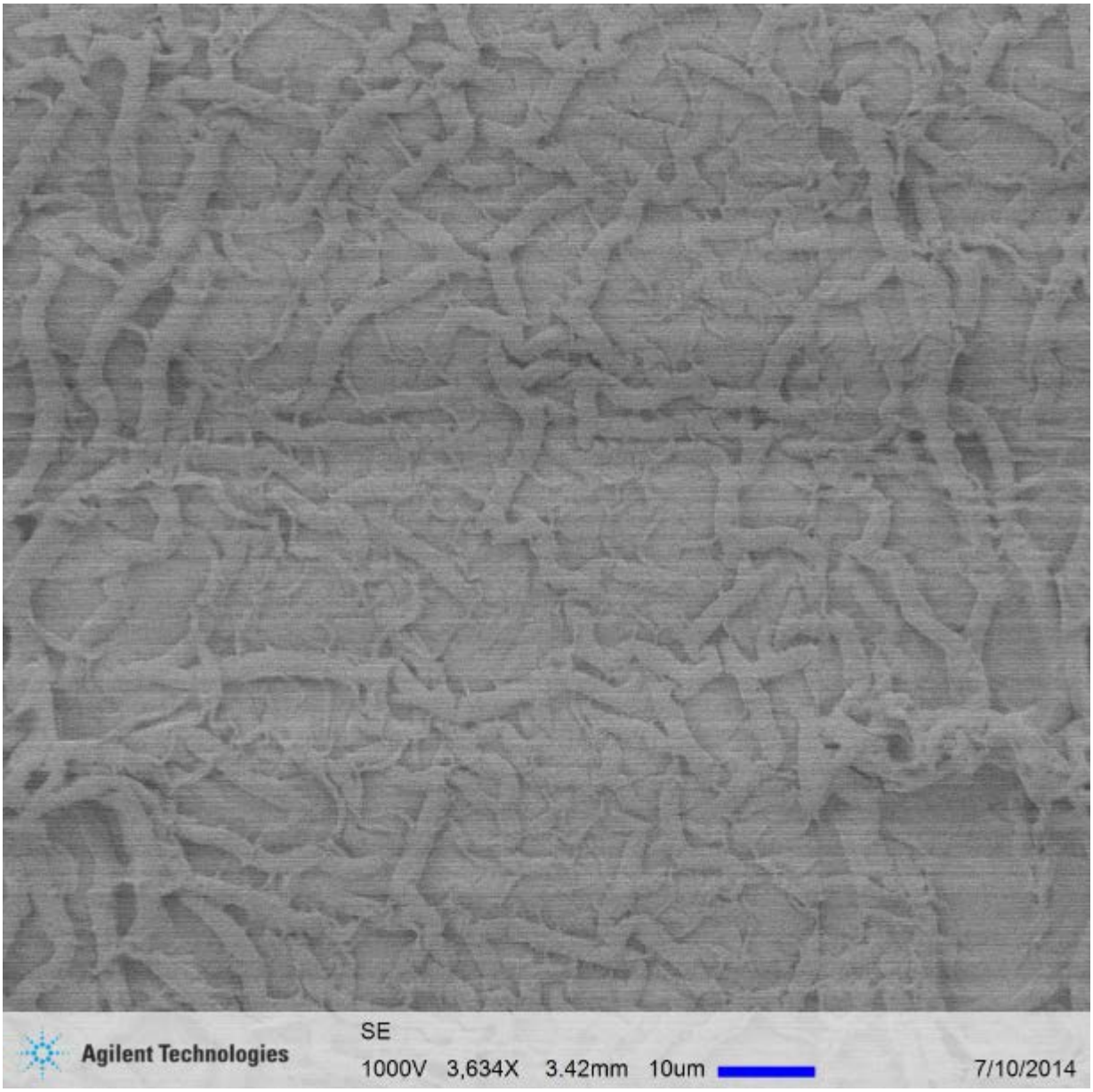

Figure 3.4 is the surface of 6 layer 3% Al:ZnO thin films synthesized using aluminum acetate and layered on piranha AB quartz. The thin film exhibits structured growth across the substrate and some overall uniformity.

Although we see a substantial increase in coverage and uniformity, there is still a defected area seen on the surface of the thin film. This also can be attributed to the nonhomogeneous solution and inconsistent layering method. One key difference between the thin films and Figures 3.3 and 3.4 is the etching procedure. This initial investigation suggests that quartz substrates pretreated in an AB piranha bath will yield films with better coverage and uniformity, but this still could be due to the lack of layers on the substrate. 6 layer 3% Al:ZnO thin films synthesized using aluminum chloride are also grown on AB quartz, yielding fairly uniform full coverage.

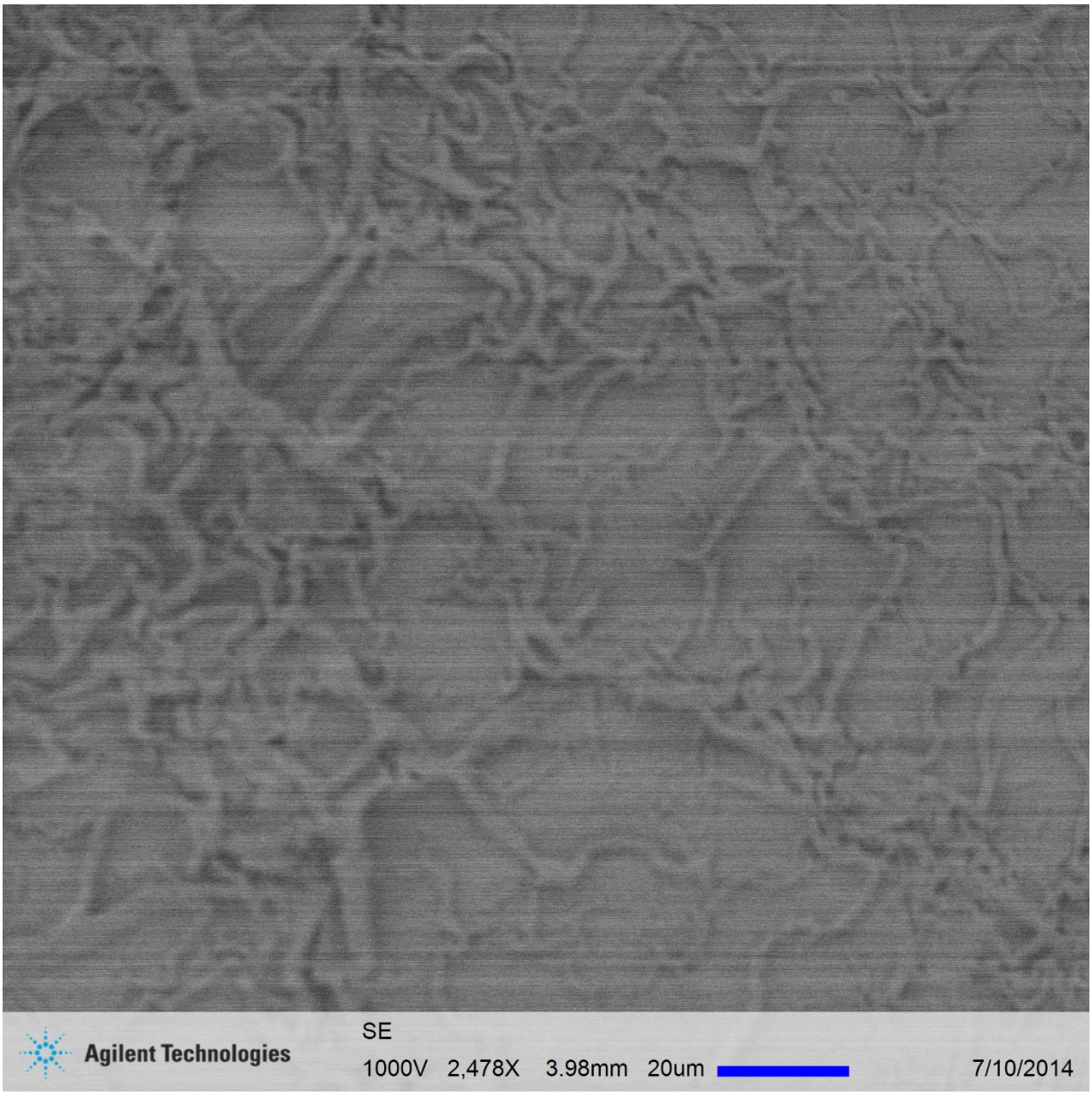

Figure 3.5 is the surface of 6 layer 3% Al:ZnO thin films synthesized using aluminum chloride and layered on piranha AB quartz. The thin film exhibits structured growth across the substrate and some overall uniformity.

Although we see structured growth of Al:ZnO, we cannot use these SEM images to compare the layering and uniformity of the two different precursor solutions, as the magnification for Figure 3.4 is 3,634x and for Figure 3.5 is 2,478x. This image merely tells us

that precursor solutions doped with aluminum chloride also yield full coverage and some uniformity on piranha AB etched quartz. The thin film synthesized from the same solution on BA etched was considered to measure the film thickness. Through various failed attempts this thin film was mistreated and highly contaminated before SEM measurements, rendering it useless for comparison.

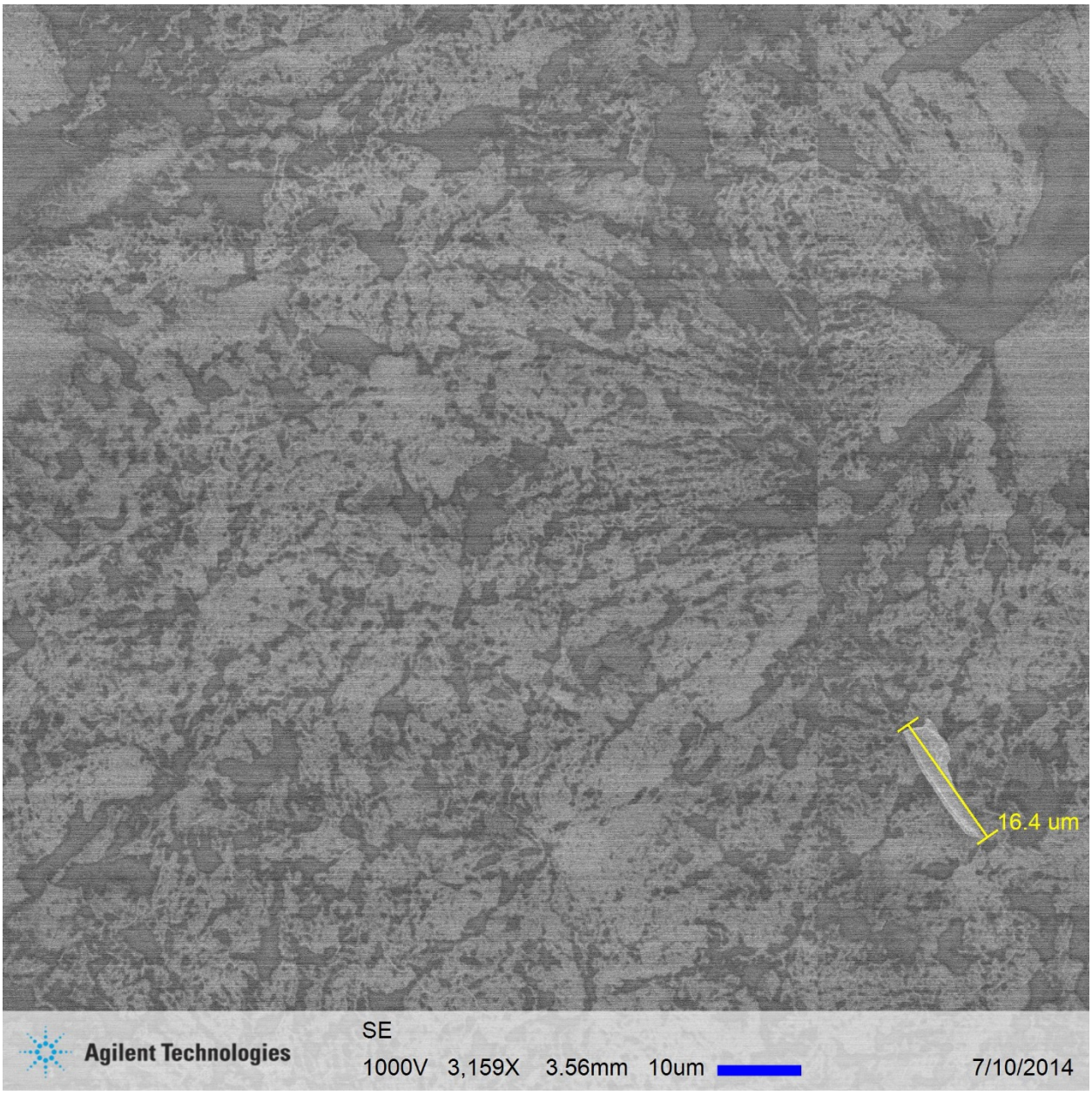

Figure 3.6 is the surface of a highly defective 6 layer 3% Al:ZnO thin films synthesized using aluminum chloride and layered on piranha BA quartz. It is an example of how sensitive these thin films are to everyday lab tools and conditions.

Although these thin films are not perfected, we have established that precursor solutions made with aluminum chloride and aluminum acetate can be used to layer zinc oxide thin films. To ensure even better coverage, the number of coatings was increased to 12 and the characterization was repeated.

3% Al:ZnO thin films with 12 layers on piranha AB quartz were of low quality, lacking overall coverage, uniformity and structure, as seen in the following figures.

(a) 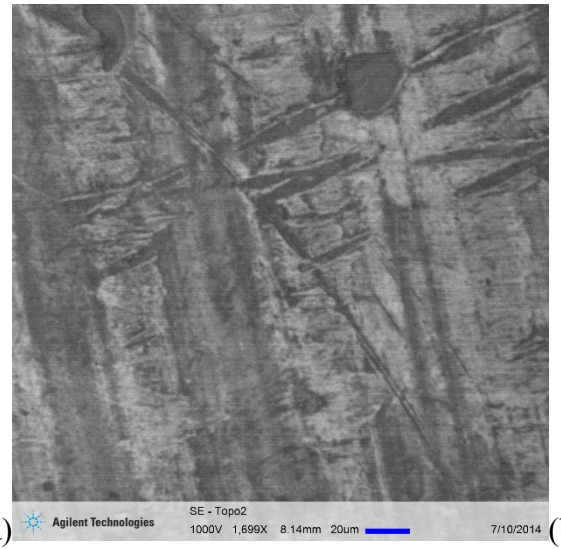

(b) 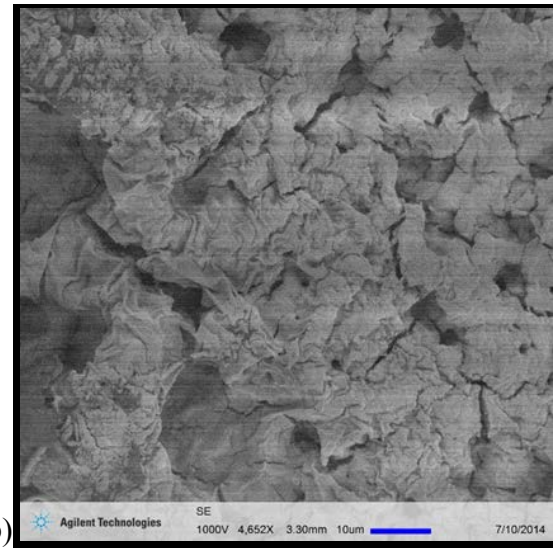

Figure 3.7 (a) is the surface of 12 layer 3% Al:ZnO from aluminum acetate precursor on piranha AB quartz (b) and 12 layer 3% Al:ZnO from aluminum chloride precursor on AB quartz. These films are discontinuous, non-uniform layering with a lack of substrate coverage and uniformity. This tells us that increasing the number of layers will not necessarily increase the thin film coverage and uniformity. To further investigate, 3% Al:ZnO thin films with 12 layers on piranha BA quartz and exhibited good coverage and overall uniformity, according to SEM.

(a) 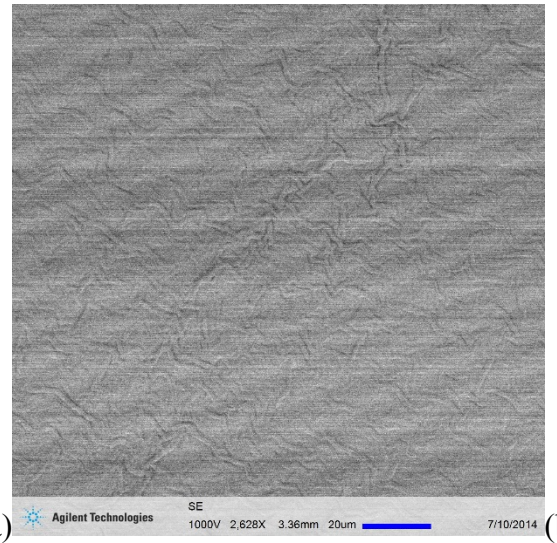

(b) 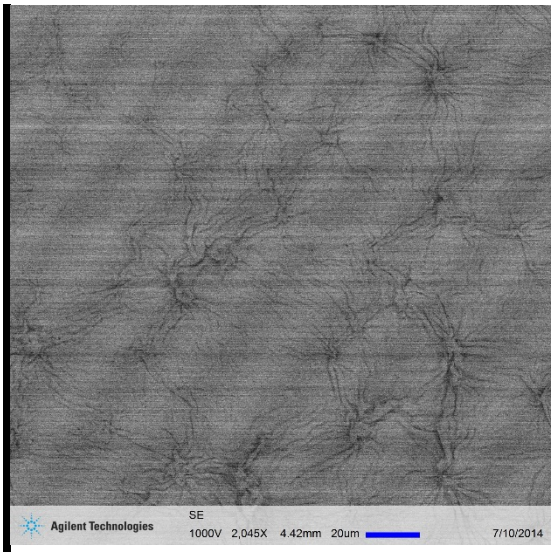

Figure 3.8 (a) is the surface of 12 layer 3%Al:ZnO on piranha BA quartz from aluminum chloride precursor (b) and 12 layer 3% Al:ZnO on BA quartz from aluminum acetate precursor. These films clearly have full coverage and uniformity with structured ZnO growth.

This contradicts previous results which show AB etched substrates are more compatible for 3% Al:ZnO thin films. Furthermore, additional layering seemed to help with uniformity and coverage for BA etched quartz substrates. Therefore, we cannot determine that one specific pretreatment method will lead to better coverage and uniformity. Although the effects of this substrate surface pretreatment technique are not fully understood, SEM results show improvement in quality on zinc oxide thin films on pretreated 1 inch diameter quartz substrates. SEM tells us we can successfully spin coat layers of 3% Al:ZnO precursor solution with both aluminum chloride and aluminum acetate.

Once it is determined that zinc oxide has been deposited on the substrates, the optical properties of these films can be observed. Before relying on technology, it is easy to see that these Al:ZnO thin films were not completely transparent and the surface very rough. Overall, they were cloudy and of yellowish color, making it hard for the human eye to see through them. Absorbance measurements are used to study the UV to visible range absorbance of the samples.

3.2.4 Optical characterization of 3% Al:ZnO thin films

Optical absorbance are applied to study the band gap of ZnO thin films. A halogen and deuterium lamp are used to create a spectrum of 190-1100 nm light. This light is passed through a monochromator to shine one wavelength of light onto a sample. A detector on the other side of the sample collects the signal that passes through the sample. The following diagram displays the setup of the spectrometer.

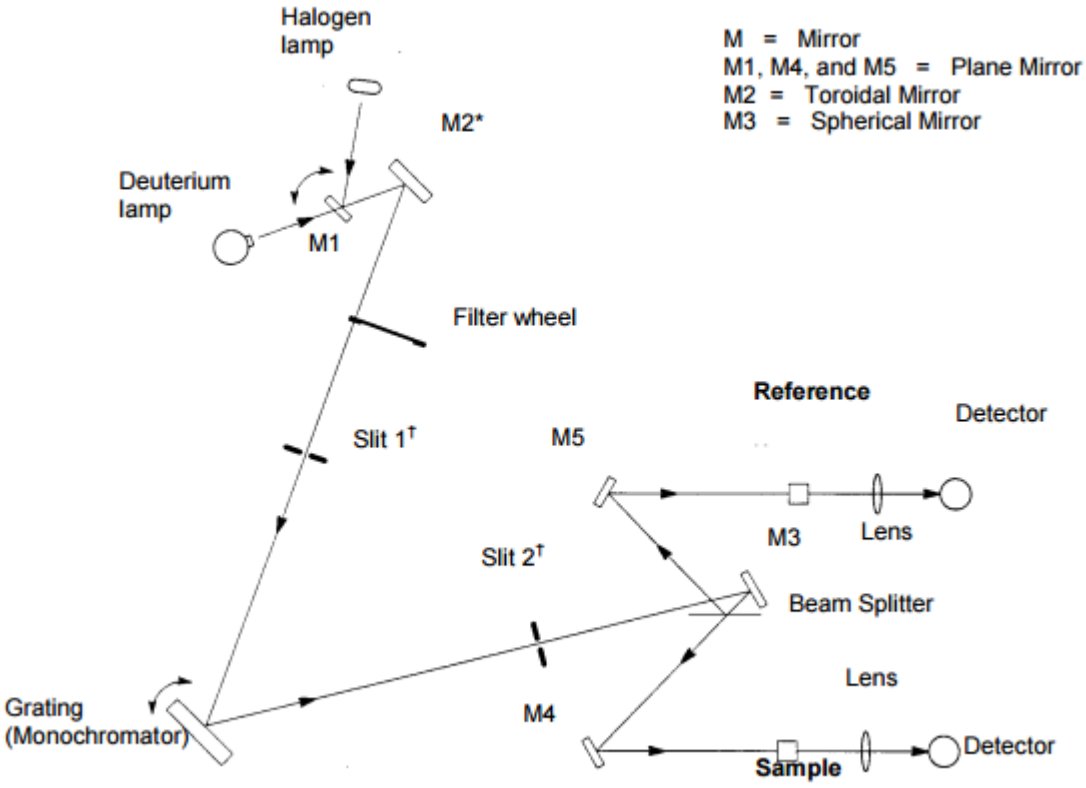

Figure 3.9 is a diagram of the layout of Perkin Elmer Lambda 35 spectrometer. A series of optics is used to shine light onto a sample to see which energies are absorbed and which are transmitted [49].

3% Al:ZnO samples were placed in the beam path for the following measurements.

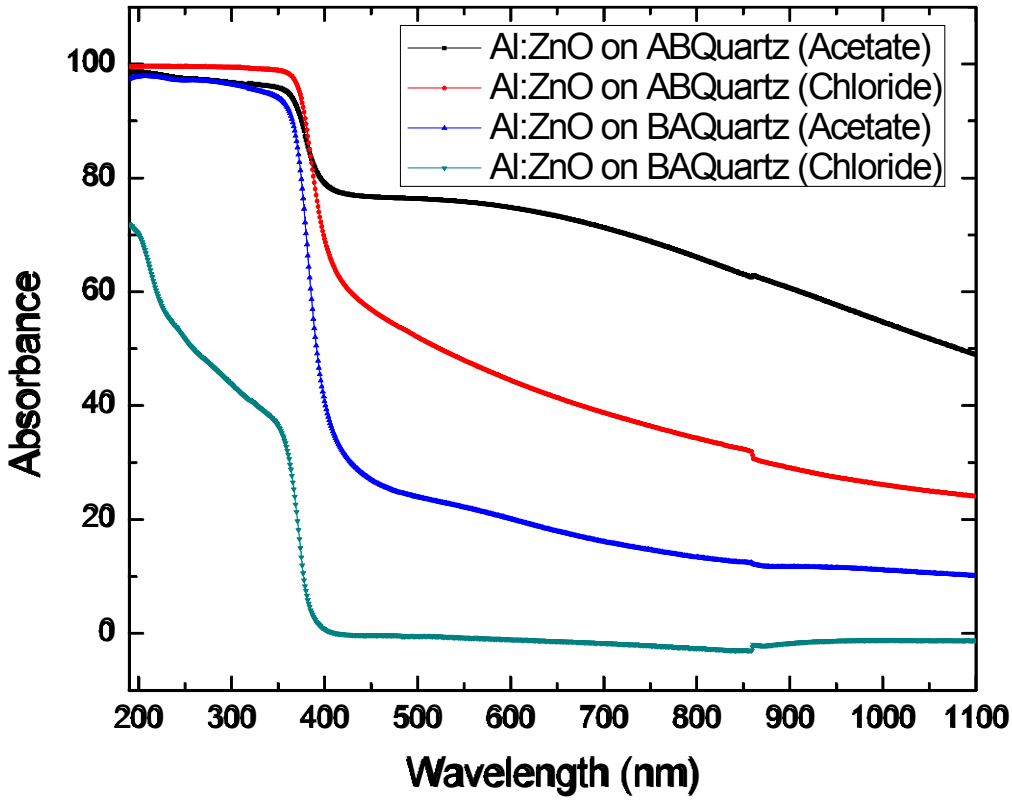

Figure 3.10 is the absorbance spectrum for 6 layer 3% Al:ZnO thin films. The band gap near 380 nm is a signature of ZnO. These samples exhibit high UV absorbance with an overall lack of transparency in the visible range.

These measurements further signify good overall coverage, with the exception of the 3% Al:ZnO sample on BA quartz synthesized from the aluminum chloride doped precursor. This was the mistreated sample and absorbance and SEM confirm that this thin film lacked coverage and layering. The other samples seem fully covered as they display full UV absorbance at energies greater than the band gap. But, these samples also exhibit substantial absorbance in the visible range. As the goal is to achieve transparent conductive oxides, the thin films should transmit visible light, rather than absorb it. Band gap defects within the thin film allow for low

energy light absorbance. Therefore absorbance measurements reveal highly defective ZnO thin films unsuitable for use as a transparent conductive oxide (TCO). These defects can also be seen in other optical techniques, such as photoluminescence.

Photoluminescence is the light emission of a material after it absorbs photons. When photons are absorbed, they excite electron-hole pairs which are free to more throughout the material. Upon relaxation these electrons can recombine with the hole, giving off radiation in the near band gap emission, or with other doping and impurities, giving off a less energetic signal.

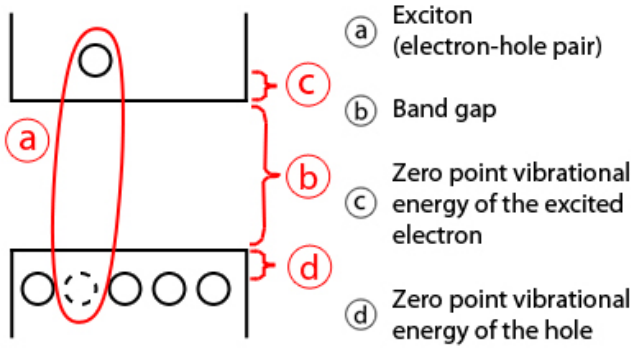

(a)

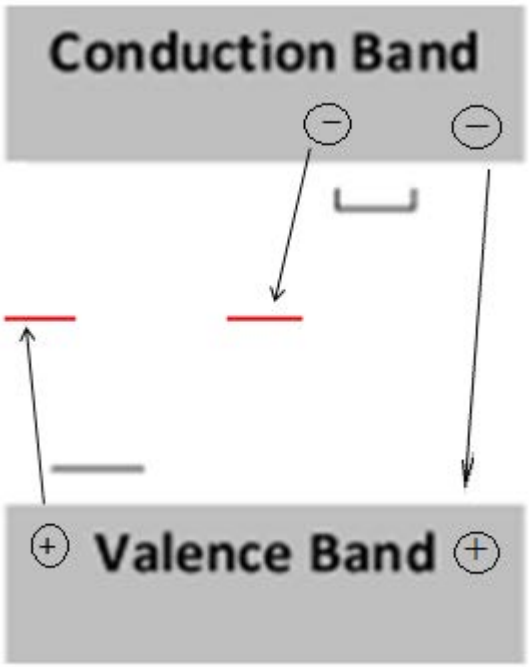

(b)

Figure 3.11 (a) shows that electron-hole excitation after a photon is absorbed and (b) depicts the recombination of the exciton with itself or other luminescence centers [50].

Photoluminescence was measured to investigate the defects of 3% Al:ZnO to yield the following luminescence signal.

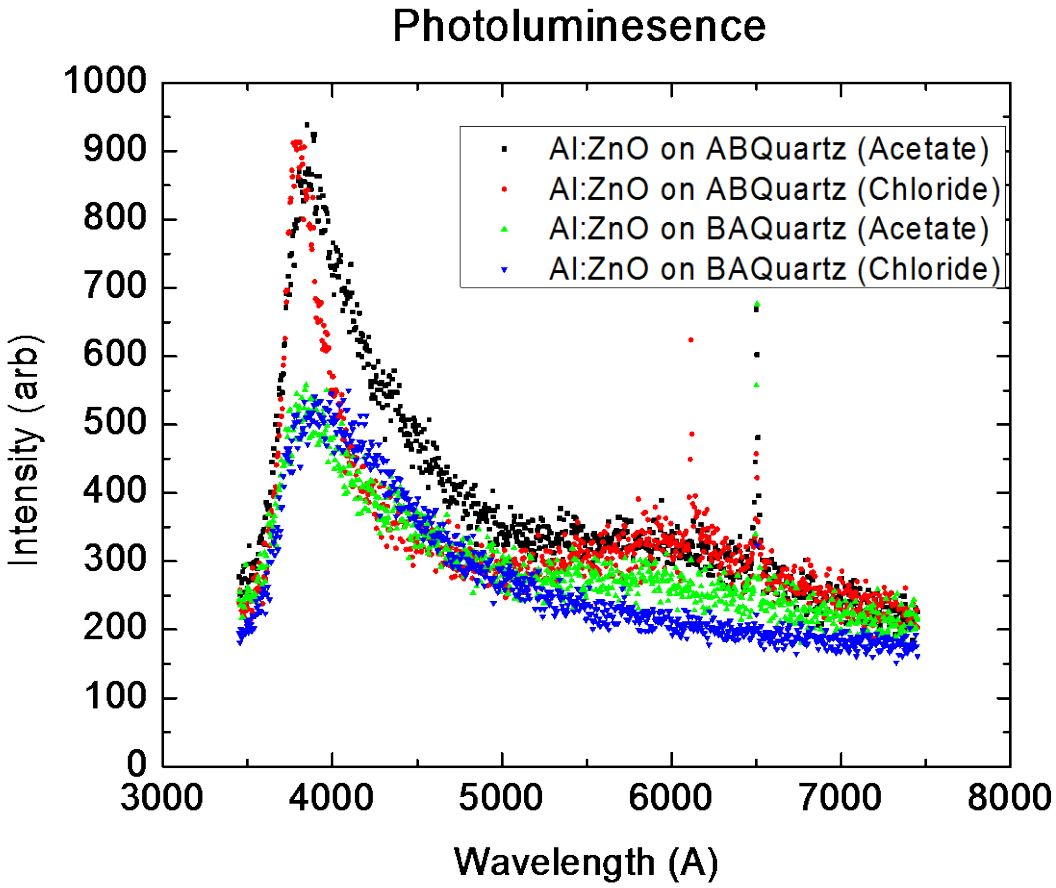

Figure 3.12 is the photoluminescence measurements for 3% Al:ZnO thin film samples. A 325nm laser was used for excitation and caused a near band emission at 3800 Å. Some samples exhibit low intensity luminescent signals in the visible range. The difference in peak height and width between samples is due to different integration times and wavelength resolutions. The peaks with half the height were measured with half the integration time and the peaks with half the width had twice the resolution.

Each sample that exhibited visible range absorbance, also showed visible range luminescence while the one sample with little visible range absorbance showed no visible range luminescence peaks. Just as visible range light is absorbed by bandgap defects, excited charge carriers can recombine with these traps, causing a luminescence signal with less energy than the band gap. This proves that the lack of transparency in these Al:ZnO thin films comes from defects changing the band structure and causing the sample to absorb lower energy light. Although one sample had high transparency and no visible luminescence, this is most certainly due to the lack of substrate coverage and mistreatment of the sample.

Although some good layering and uniformity has been achieved, visible range absorbance and photoluminescence signals are a good sign that the 3% Al:ZnO thin films are too defective for use as a TCO.

3.2.5 Conclusions

The sol-gel spin coating technique was used to deposit 3% Al:ZnO thin film layers onto pretreated 1 inch quartz substrates. Although some solutions were not completely mixed, SEM tells us that the larger size and piranha etching procedures improve compatibility with the substrate and solution. Evidence shows both procedures can be used to yield better overall coverage and uniformity than untreated 10x10mm sapphire.

Optical measurements show that zinc oxide thin films are highly defective. The favored candidate for this is the temperature change, as the substrate goes through a number of heating stages. For example, when the substrate was placed on the hot plate to dry, the visible range absorbance changed. The boiling point of the solvent is 125^{o}C, so it could be true that the drying temperature can be decreased from 210^{o}C to reduce defects from thermal shock. Also, a hot substrate can evaporate solvent from the solution during the layering process. This will yield

thick and inconsistent films with many structural defects. From this point, thin films are dried in an oven at 150^{o}C in an effort to reduce temperature shock effects, but still completely evaporate the solvent.

Overall, these films cannot be used as a TCO because of minimal visible range transparency and a large number of luminescent defects but, valuable information was learned about the sol-gel spin coating technique. With this knowledge, the technique was further optimized in an effort to obtain high quality zinc oxide thin films.

3.3 An Optimized Sol-gel Spin Coating Method for ZnO Thin Films

After the second attempt to synthesize high quality zinc oxide thin films, it was learned that various steps in the procedure are highly dependent on temperature. To ensure control, the solution and each thin film layer is cool to room temperature after any thermal treatment to prepare for spin coating. Also, the drying temperature is reduced to 150^{o}C to better control structural defects.

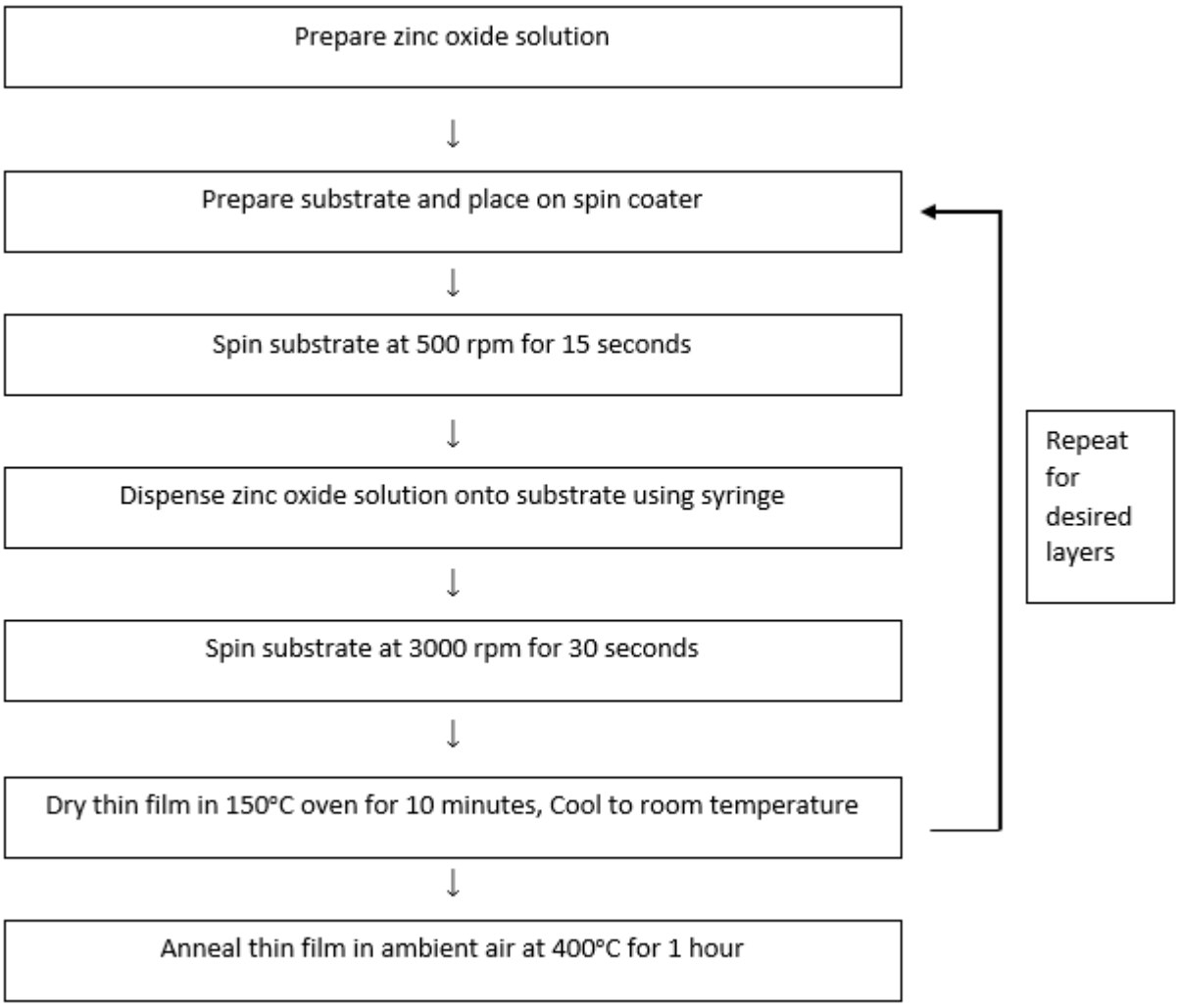

Figure 3.13 summarizes the optimized sol-gel spin coating method used in an effort to improve ZnO thin film qualities. The key changes are to monitor the precursor solution and to dry the film at a less extreme but effective temperature and cooling it to room temperature before the next layer.

3.3.1 Sol-gel Synthesis of Doped and Undoped ZnO Thin Films

In summary, a precursor solution is prepared to maximize transparency by dissolving the aluminum salt completely. Aluminum nitrate has a high solubility, similar to aluminum chloride, and it is used as a dopant for Al:ZnO precursor solutions and gallium nitrate is used as a dopant to for Ga:ZnO precursor solutions for comparison. These solutions are doped with 1% aluminum or gallium nitrate, heated to 60^{o}C, stirred for 2 hours and cooled to room temperature to prepare for layering.

The substrates are prepared with piranha AB and BA etching procedures to clean residual impurities and create a compatible surface for the precursor solutions. For the most part, one etching procedure did not play a significantly greater role in the synthesis process than the other and eventually the piranha AB etch is more commonly used to pretreat quartz. These room temperature substrates begin spinning at 500 rpm and 30-50 drops of solution is manually dispensed by a syringe. Enough solution must be dispensed to fully cover the substrate while minimizing waste. The substrate and solution then accelerate to 3000 rpm to spread and remove excess solution to obtain a smooth gel-like zinc oxide thin film.

This gel-like thin layer of zinc oxide is placed in an oven at 150^{o}C for 10 minutes to remove the remaining solvent to yield a solid zinc oxide layer. The thin film is removed from the oven and cooled to room temperature to prepare for another layer of precursor solution and round of drying. This process is repeated for 12-16 layers to ensure coverage and consistency. After multiple layers, thin films are thermally treated in ambient air at 400^{o}C for 1 hour to enhance the structural properties.

3.3.2 SEM Characterization

During this synthesis process, it was clear to see with the naked eye, that thin films were being deposited onto the pretreated quartz. To confirm, lowly resolved SEM measurements of the surface of 16 layer 1% Al:ZnO show full coverage and some overall consistency and uniformity.

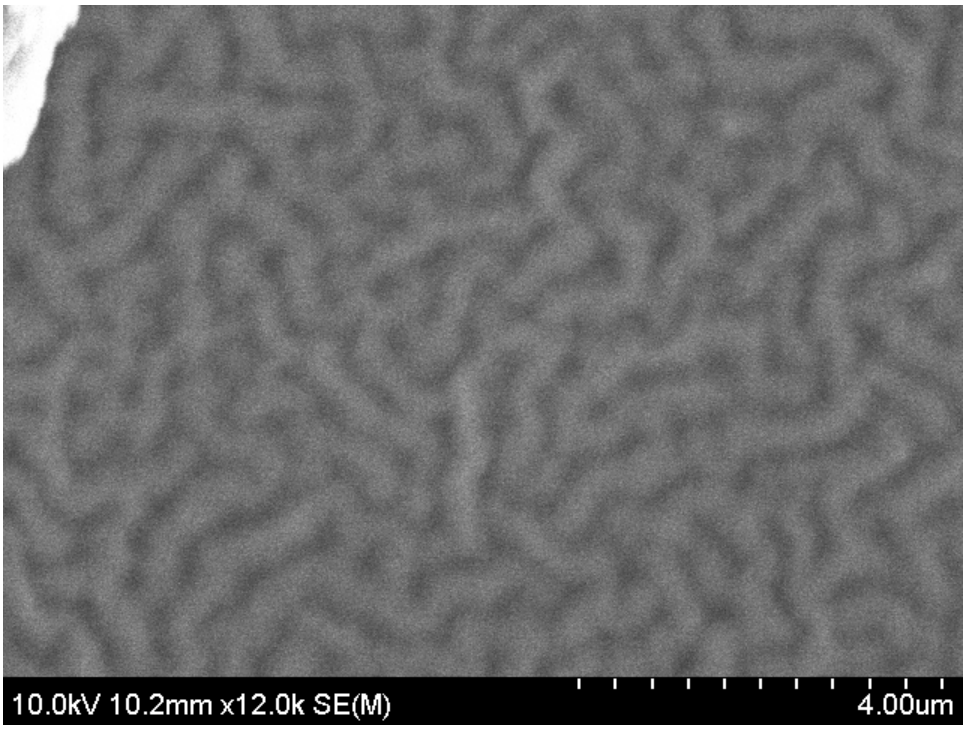

Figure 3.14 is the surface of 16 layer 1% Al:ZnO thin films synthesized by the optimized sol-gel spin coating technique on piranha AB quartz. The thin film exhibits structured growth across the substrate and some overall uniformity.

Also, more resolved SEM reveals improved quality and better overall coverage for other ZnO thin films synthesized using the latest technique.

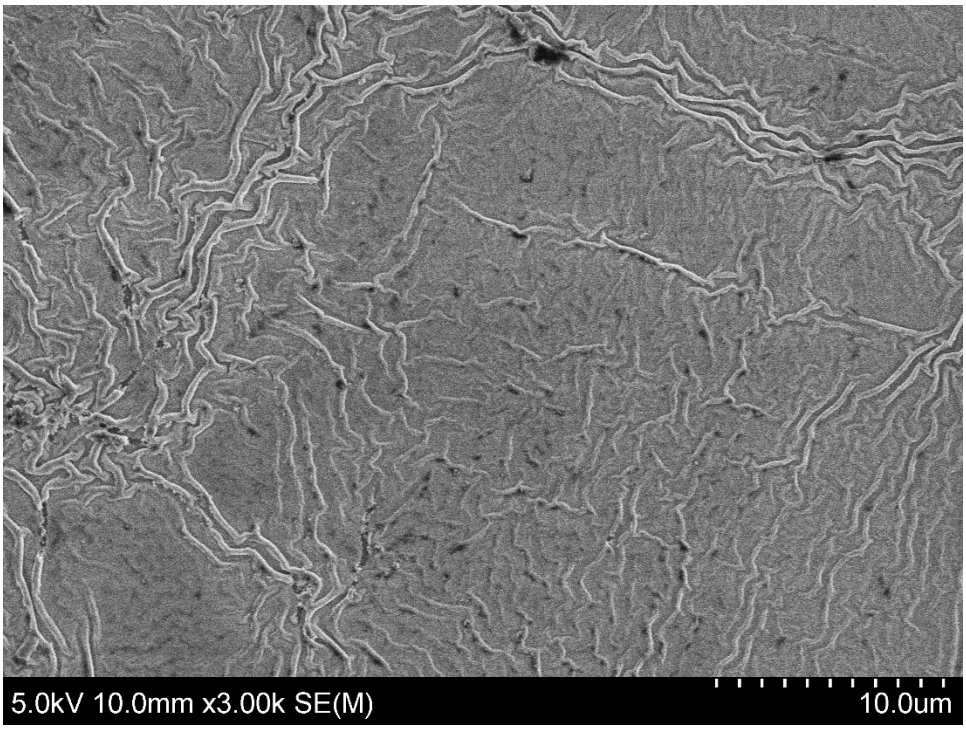

Figure 3.15 is the surface of 16 layer 3% Mn:ZnO thin films synthesized by the optimized sol-gel spin coating technique on piranha AB quartz. Some defects and inconsistencies are noticed, but the thin film exhibits structured growth across the substrate and some overall uniformity.

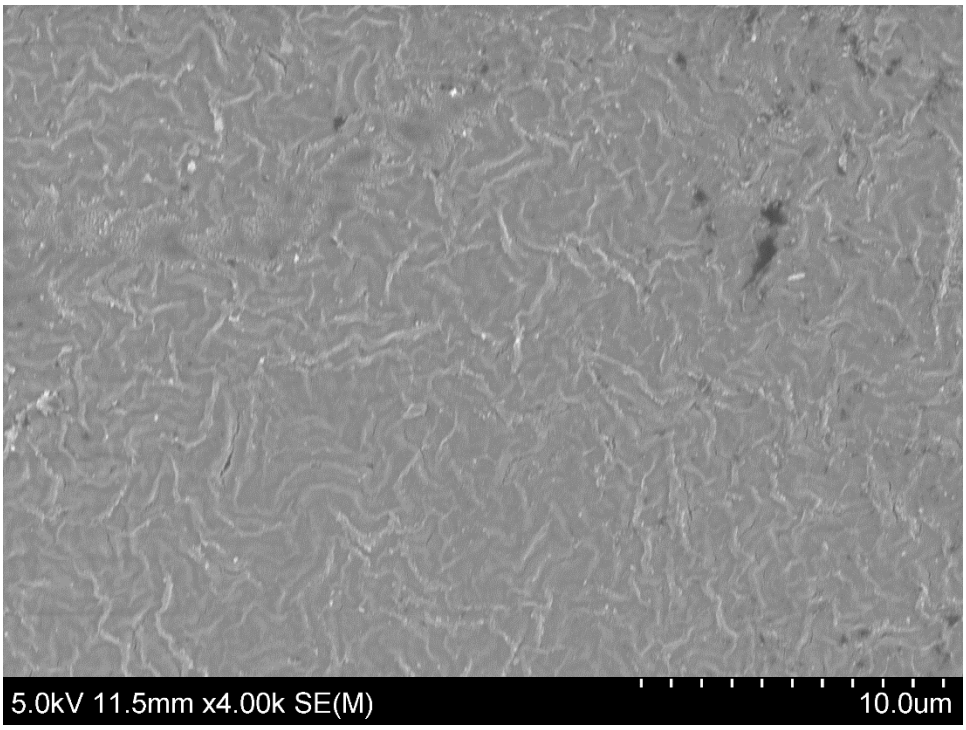

Figure 3.16 is the surface of 16 layer 1% Co:ZnO thin films synthesized by the optimized sol-gel spin coating technique on piranha AB quartz. Even with obvious surface defects, we see full coverage, structured growth and some overall uniformity.

SEM was also used to measure a rough estimate of the thickness of 16 layer 1% Al:ZnO.

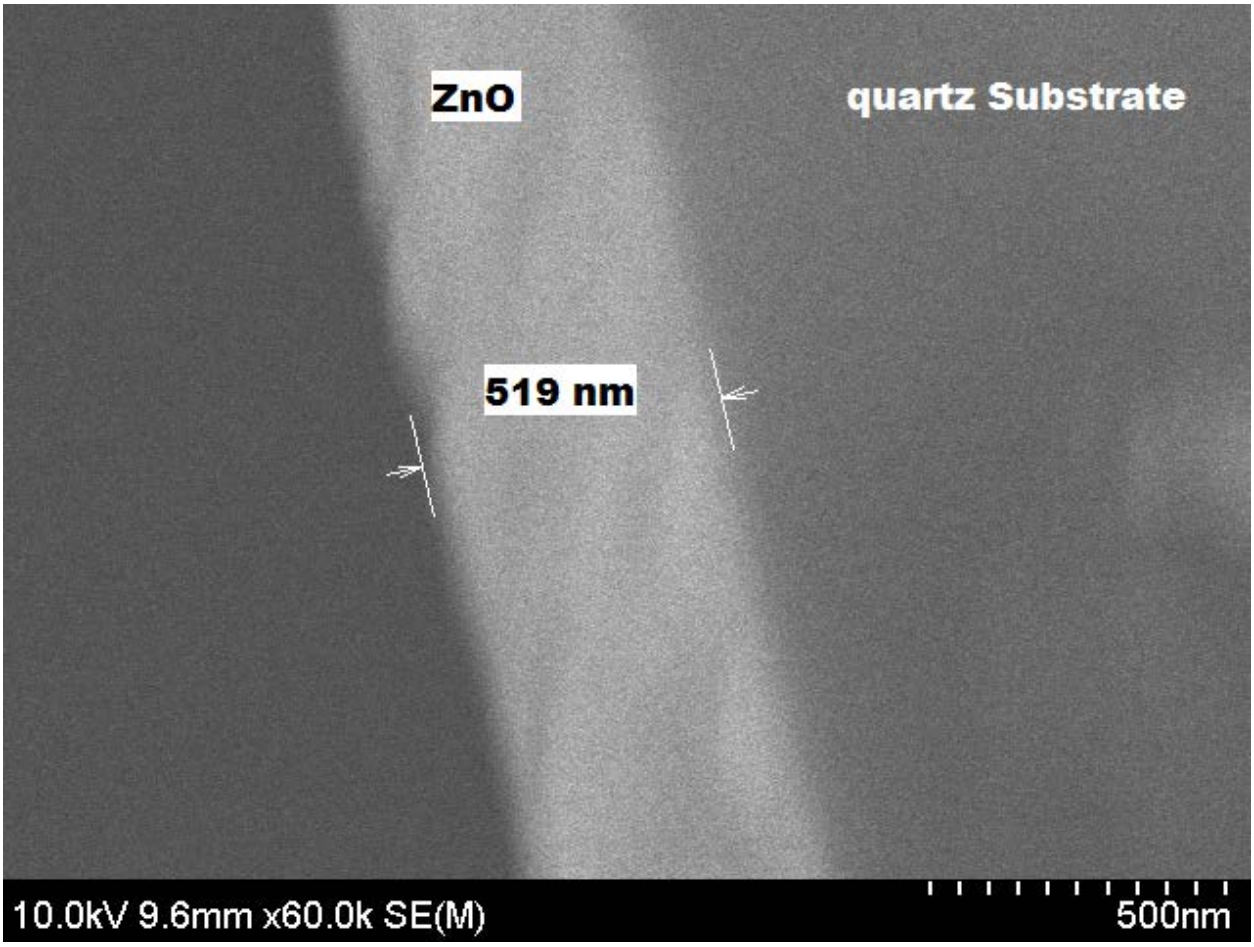

Figure 3.17 is the side-view of 16 layer 1% Al:ZnO thin film to measure thickness. The sample was cut and stood vertically in the SEM allowing us to see the face-view of the cut. The substrate and thin film could be differentiated to measure a rough thickness of t = 519 nm. Therefore, the thickness of each layer of zinc oxide is about l = 32.44 nm. We will multiply this value by the number of layers of the films investigated to estimate the thickness.

Even without these SEM measurements of the thin film surface, there is evidence full substrate coverage is achieved and these doped and undoped zinc oxide thin films are subject to absorbance and XRD measurements to investigate the optical and structural properties.

3.3.3 Optical Characterization

Undoped and 1% Al:ZnO thin films were synthesized using the newest sol-gel technique were investigated using absorbance measurements.

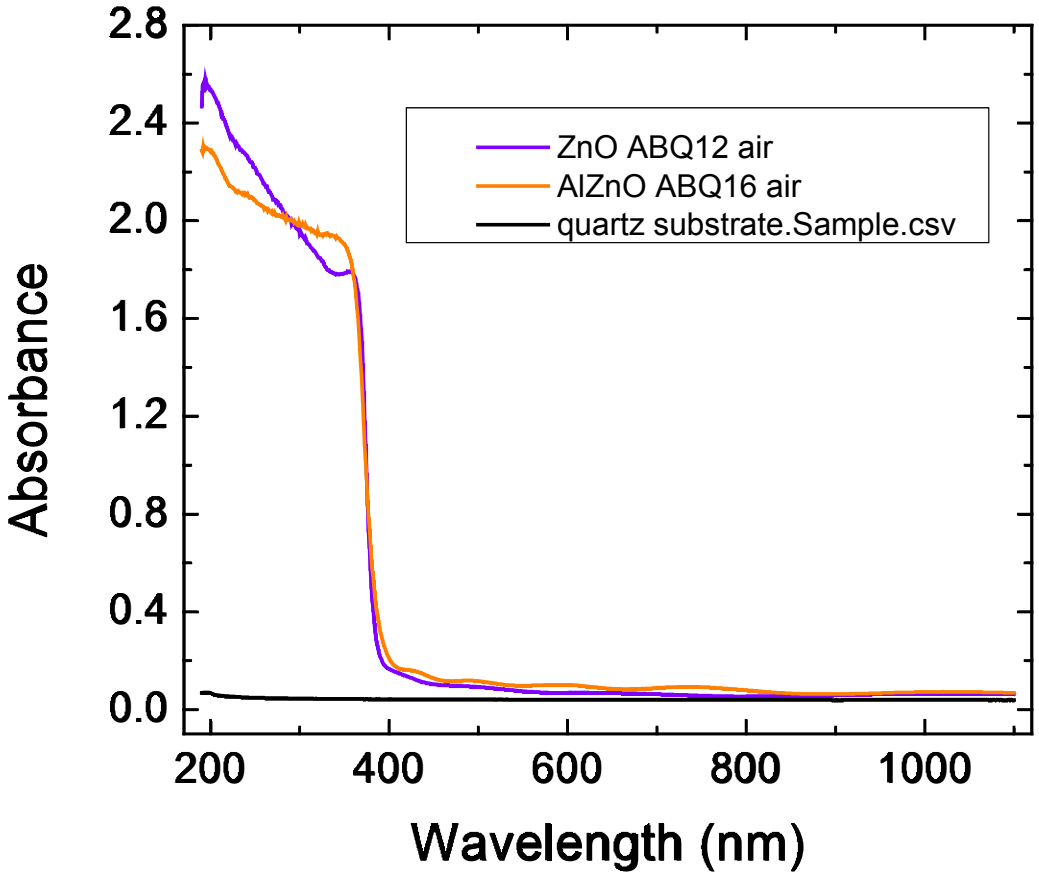

Figure 3.18 is the absorbance spectra of 12 layer undoped ZnO on AB etched quartz, 16 layer 1% Al:ZnO on AB etched quartz, and the quartz substrate itself. The ZnO films were annealed in air at 400ºC for 1 hour after the final layer. They exhibit strong UV absorbance with a band gap close to 380 nm, the signature for ZnO.

If we analyze the UV range absorbance, we see that the Al:ZnO sample absorbs more at the band gap energy because it has 4 more layers. These sample spectra cross in the UV

absorbance range due to some reflectance or other phenomena. Both curves show an increase in absorbance with photon energy, but the aluminum doping reduces this rate significantly. High transparency in the visible range for both samples is a good sign that band gap defects have been minimized and film quality improved.

3.3.4 XRD Characterization

An X-ray diffractometer was used to collect crystal patterns of doped and undoped ZnO thin films. Substrates with thin film layers were placed on a stage and struck with x-rays to obtain 2θ diffraction angles. ZnO samples synthesized using the optimized sol-gel method have visible peaks for many crystal phases. X-ray Diffratction (XRD) patterns for ZnO and Al_2O_3 must be considered for comparison as secondary phases can form during synthesis.

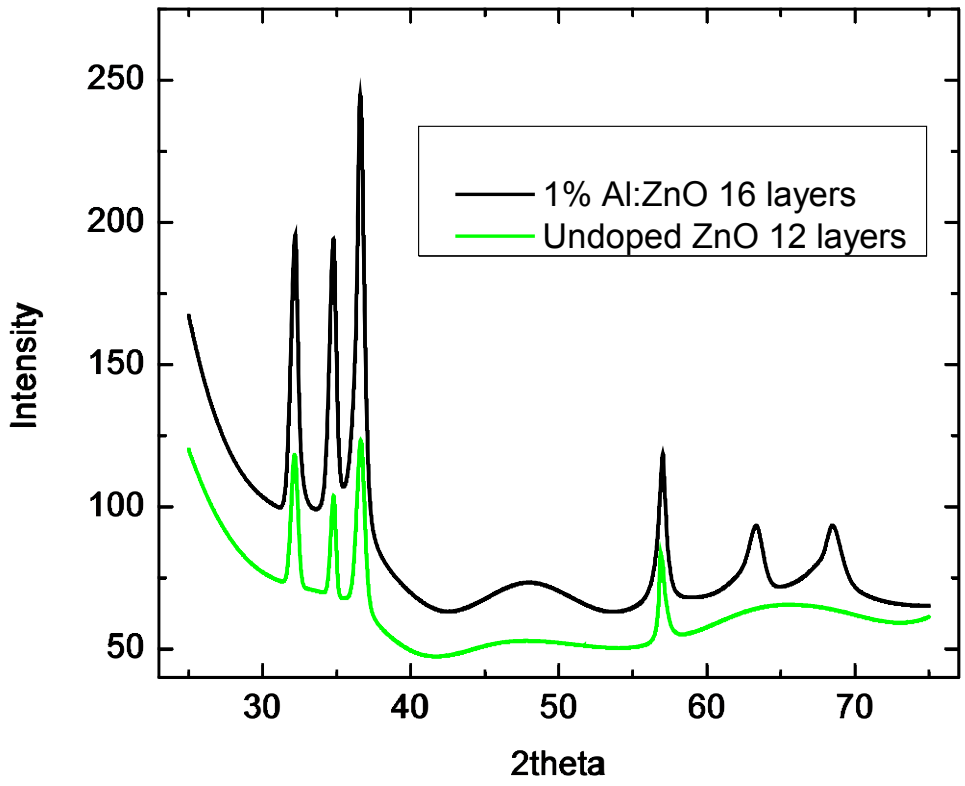

Figure 3.19 shows the XRD patterns for 12 layer undoped ZnO on AB etched quartz and 16 layer 1% Al:ZnO on AB etched quartz and annealed in ambient air at 400°C for 1 hour. Both exhibit a polycrystalline structure and the crystal patterns for ZnO and Al_2O_3 can be referred to in Appendices B and C.

Table 3.2 XRD peak positions, separation and phase for undoped and 1% Al:ZnO thin films synthesized by sol-gel spin coating. References for orientation of ZnO and Al_2O_3 are found in Appendices B and C.

Undoped ZnO					1% Al:ZnO				
Peak No.	2θ (deg)	St. Dev. of 2θ	d(Å)	St. Dev. of d	Peak No.	2θ (deg)	St. Dev of 2θ	d(Å)	St. Dev of d
1	32.1284	0.046488	2.78367	0.003916	1	32.189	0.036345	2.77857	0.003051
2	34.7698	0.058412	2.578	0.00419	2	34.7579	0.036356	2.57886	0.002611
3	36.5966	0.045843	2.4534	0.002964	3	36.5423	0.02436	2.45693	0.001581
4	56.8583	0.040617	1.61799	0.001059	4	57.0102	0.039321	1.61404	0.001019
					5	63.277	0.051512	1.46844	0.00107
					6	68.4138	0.147153	1.37016	0.002582

Both of these thin films exhibit three strong peaks near 32°, 34°, and 36° which are signatures for (100), (002), and (101) phases for ZnO, respectively and the peaks near 57° and 63° (110) and (103) phases, respectively. Peak number 6 for the 1% Al:ZnO sample does not match with the index for ZnO and we do not expect it to be a large shift from the peak near 69°C. If we compare it to the index for Al_2O_3, we see that it matches the (300) crystal phase. Although it is uncertain, this peak could be from the formation of a secondary phase of Al_2O_3. From Figure 3.19 and Table 3.2, we see that the sol-gel spin coating method yields polycrystalline ZnO thin films. All respective peaks shifts are within error, leading us to believe that an aluminum doping concentration as little as 1% will only have a small effect on peak positions.

3.3.5 Conclusions

The sol-gel spin coating method most recently discussed has successfully synthesized uniform highly transparent, polycrystalline doped and undoped zinc oxide thin films. This method has successfully achieved high-quality thin films with tunable properties by the incorporation of aluminum as a dopant. The aluminum doping has little to no effect on the XRD peak positions of ZnO, but could form a secondary phase of Al_2O_3. Although the transparency and uniformity is greatly improved by the optimized sol-gel spin coating, the thin films are too resistive for two-probe resistance measurements. Therefore, they are not suitable for a TCO. But, the zinc oxide structure is still littered with defects which can be manipulated using various heat treatment techniques to tune the electronic properties for use as a transparent conductive oxide.

3.4 Hydrogen Annealing Treatment and Effects on materials properties

Annealing will greatly affect the material properties of the zinc oxide thin films, especially in hydrogen atmosphere. In ZnO, hydrogen acts strictly as a donor and zinc can fill vacancies and form interstitials with evidence for increasing the intrinsic n-type conductivity. Some undoped, 1% Al-, and 1% Ga-doped zinc oxide films are subject to post-synthesis annealing in hydrogen at 400^{o}C for 1 or more hours at various pressures in an effort to increase conductivity without greatly affecting the film structure or transparency. First, absorbance measurements help characterize the optical properties of these films.

3.4.1 Optical Characterization and Positron Spectroscopy

The following 1% Al:ZnO absorbance spectra will help us analyze the effects of annealing in hydrogen.

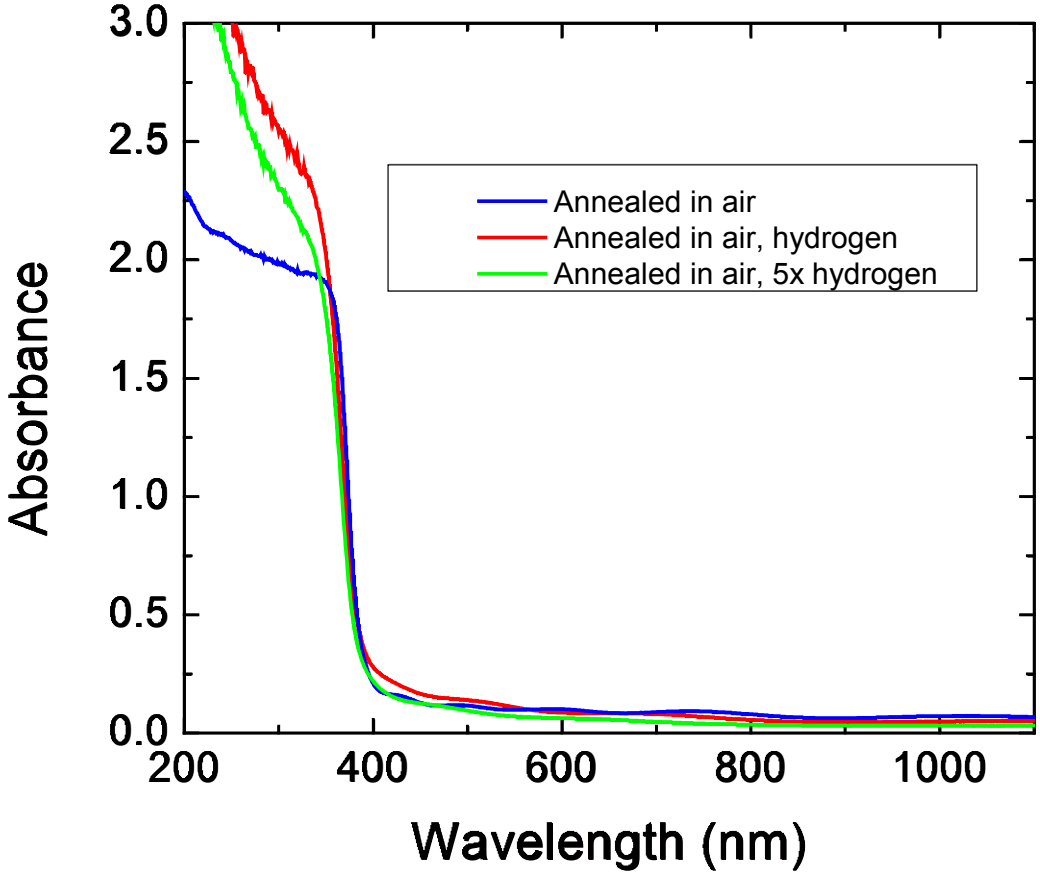

Figure 3.20 is the absorbance spectra of 16 layer 1% Al:ZnO on AB etched quartz. The Al:ZnO film was annealed in air at 400ºC for 1 hour after the final layer then cut into pieces using a diamond saw to anneal other pieces in H_2 at 400ºC for 1 hr. One sample was annealed in a higher pressure of H_2.

These thin films all exhibit strong UV absorbance with a band gap near 380 nm. Again we see a change of absorbance in the UV range due to some reflectance or other phenomena. Both curves show an increase in absorbance with photon energy, but in this case the introduction of hydrogen significantly increases the slope. High transparency in the visible range for all samples is a good sign that band gap defects remain minimized and film quality preserved.
A closer look at the visible range absorbance of these 1% Al:ZnO samples shows the effects of hydrogen.

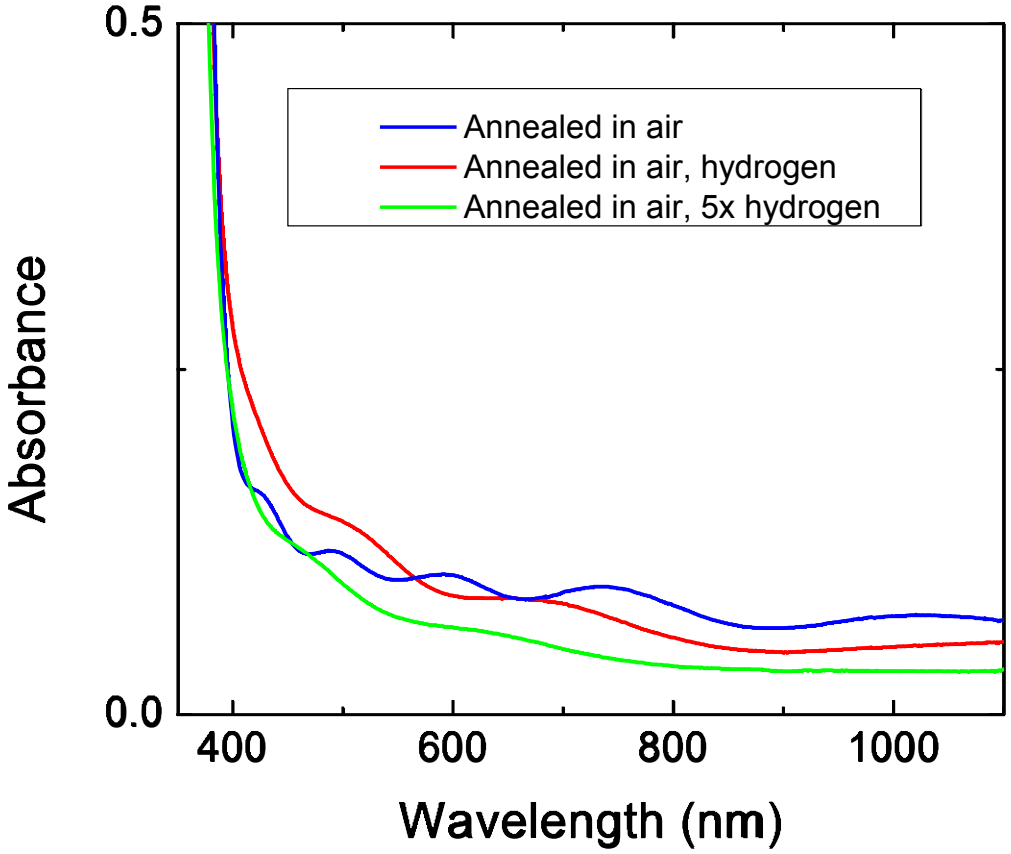

Figure 3.21 is the visible range absorbance, where there is a general decrease in absorbance as the hydrogen concentration increase.

This could be due to hydrogen filling acceptor vacancies, such as zinc, and preventing absorbance. To study the passivation of zinc vacancies, positron annihilation spectroscopy can be used. Measurements were performed to compare Al:ZnO thin films before and after annealing in a forming gas (4% H_2:96% N_2) at 400ºC for 1 hour.

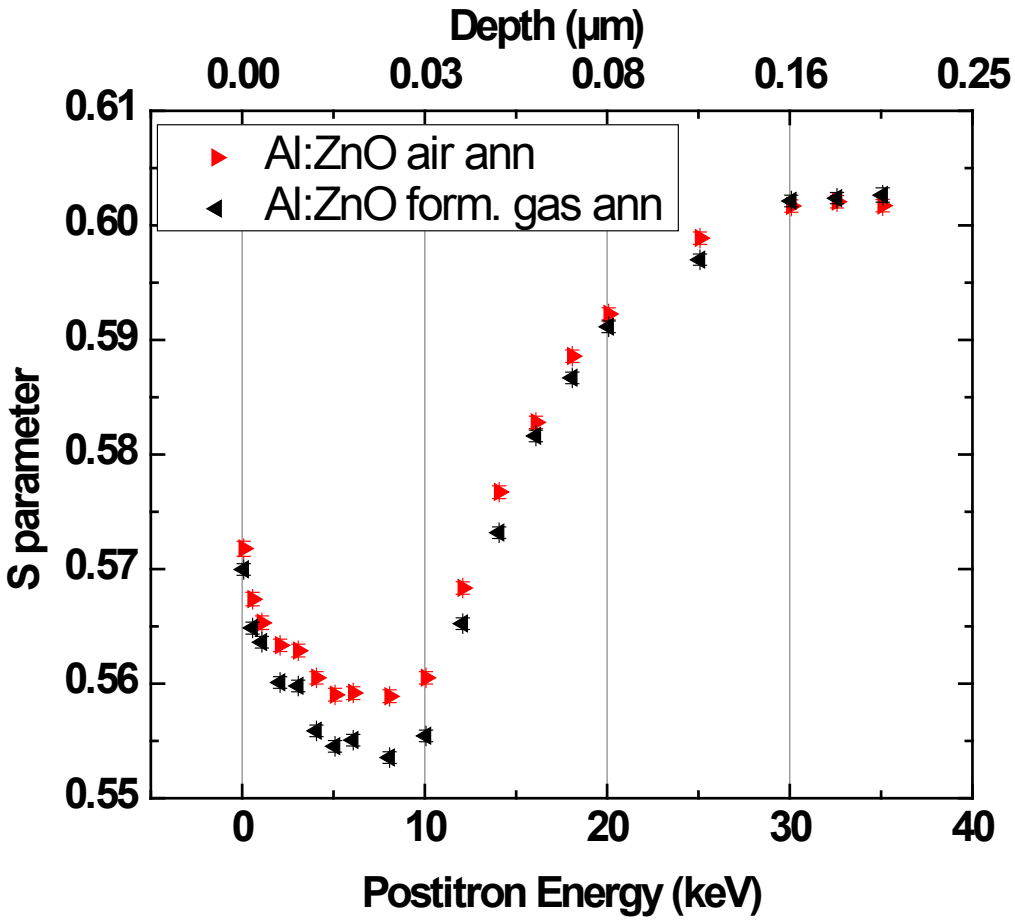

Figure 3.22 shows a decrease in the defect parameter, indicating a lower concentration of zinc vacancies. As nitrogen does not effectively interact with ZnO, it is determined that hydrogen is the reason for passivation and reduced positron trapping.

These two spectroscopy techniques indicate there could be a structural change in ZnO after treatment in hydrogen.

3.4.2 XRD Characterization

By incorporating hydrogen into the material, we see a definite effect on the material properties. The following XRD measurements can provide more insight on how hydrogen affects the structure of the material.

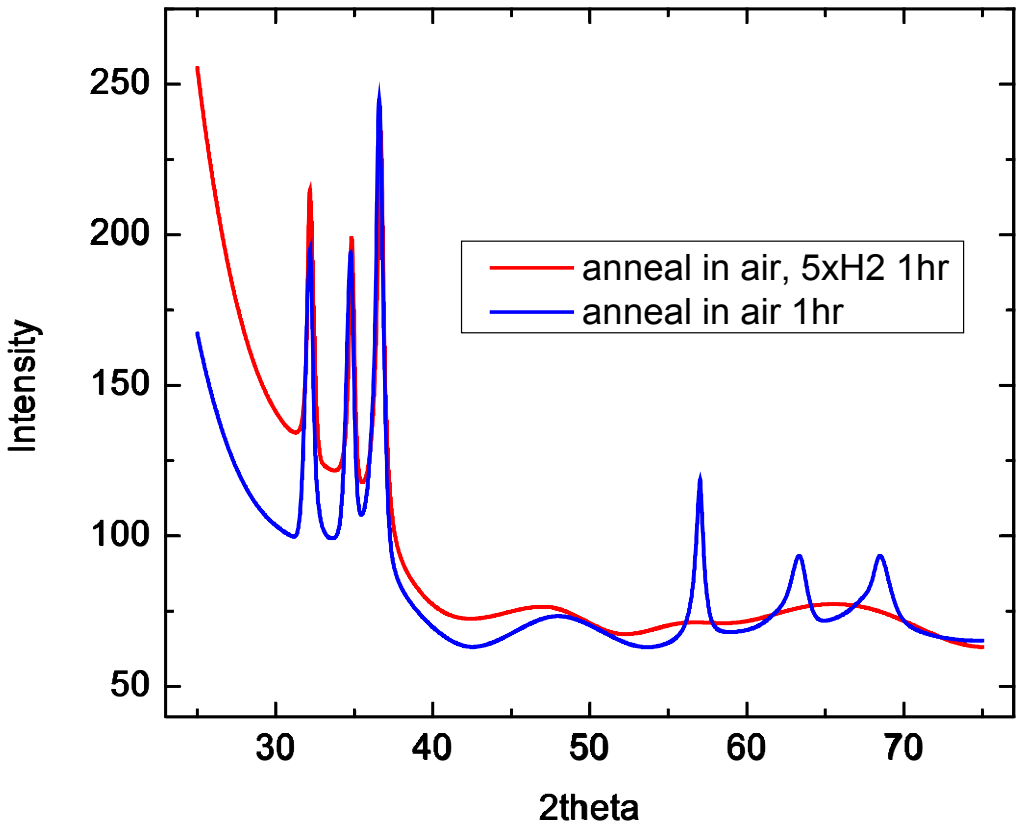

Figure 3.23 shows the XRD patterns for 16 layer 1% Al:ZnO on AB etched quartz before and after hydrogen treatment. Both exhibit a polycrystalline structure and the crystal patterns for ZnO and Al_2O_3 can be referred to in Appendices B and C.

Table 3.3 XRD peak positions, separation and phase for 16 layer 1% Al:ZnO on AB etched quartz before and after hydrogen treatment synthesized by sol-gel spin coating.

1% Al:ZnO					1% Al:ZnO, Hydrogen treatment				
Peak No.	2θ (deg)	Stand Dev of 2θ	d(Å)	Stand Dev of d	Peak No.	2θ (deg)	Stand Dev of 2θ	d(Å)	Stand Dev of d
1	32.189	0.036345	2.77857	0.003051	1	32.1095	0.022474	2.78527	0.001897
2	34.7579	0.036356	2.57886	0.002611	2	34.7975	0.046161	2.57602	0.003307
3	36.5423	0.02436	2.45693	0.001581	3	36.6578	0.037658	2.44944	0.002427
4	57.0102	0.039321	1.61404	0.001019					
5	63.277	0.051512	1.46844	0.00107					
6	68.4138	0.147153	1.37016	0.002582					

Both of these thin films exhibit three strong peaks for the signature (100), (002), and (101) phases for ZnO. After an annealing treatment in H_2 at 400°C for 1 hour, the less intense phase peaks are no longer seen. The most reasonable explanation has to do with the length of annealing. As the film is treated for a longer period of time, it becomes more crystalline. Also, just as we have seen with the low doping concentration, this treatment in hydrogen does shift in the XRD peak positions slightly, but the shift is within error, and insignificant.

To compare, 1% Ga:ZnO thin films are treated in various hydrogen atmospheres and measured using XRD. Both films were subject to the same treatment in H_2 at 400°C for 1 hr. One sample was then treated in H_2 at 400°C for 3 hours and finally in twice the H_2 pressure at 400°C for 1 hour.

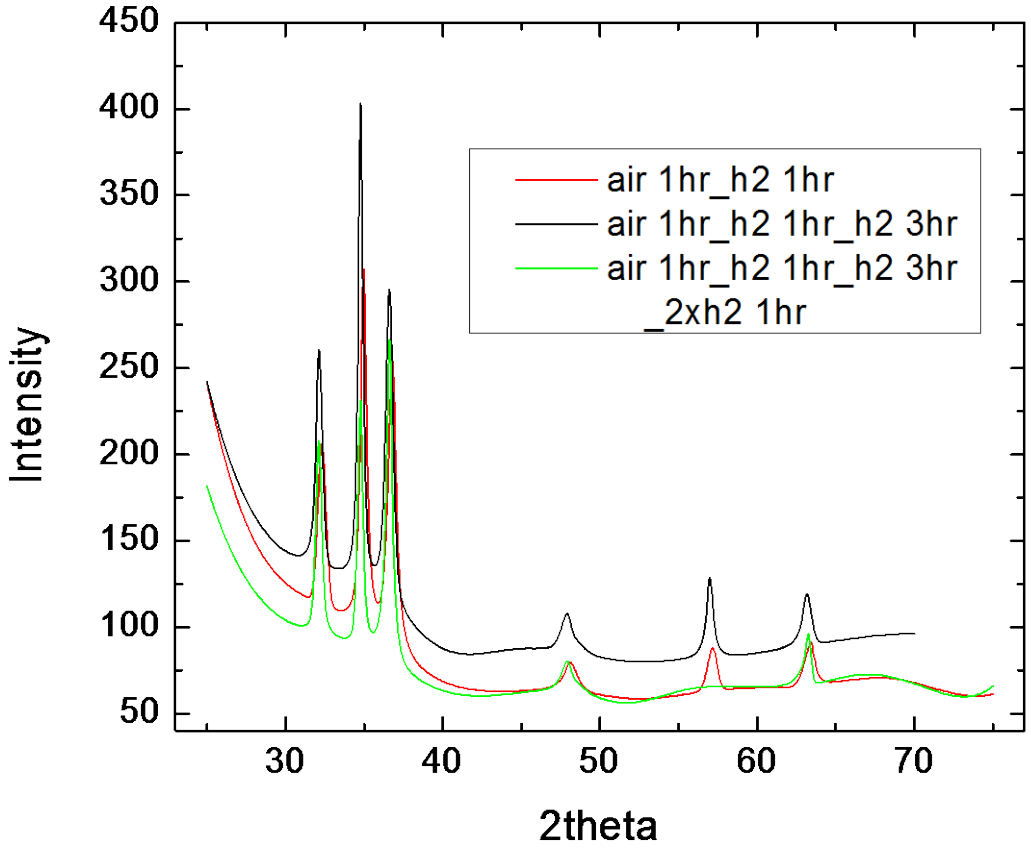

Figure 3.24 shows the XRD patterns for 16 layer 1% Ga:ZnO on AB etched quartz before and after various hydrogen treatments. All exhibit a polycrystalline structure and the crystal patterns for ZnO and Al_2O_3 can be referenced in Appendices B and C.

Table 3.4 XRD peak positions, separation and phase for 16 layer 1% Ga:ZnO on AB etched quartz, annealed in different hydrogen pressures.

1% Ga:ZnO, Hydrogen treatment					1% Ga:ZnO, Hydrogen treatment (2x pressure)				
Peak No.	2θ (deg)	ESD of 2θ	d(Å)	ESD of d	Peak No.	2θ (deg)	ESD of 2θ	d(Å)	ESD of d
1	32.0996	0.031311	2.7861	0.002644	1	32.1075	0.029842	2.78544	0.002518
2	34.7016	0.008226	2.58291	0.000593	2	34.7573	0.027991	2.57891	0.002011
3	36.5683	0.023943	2.45523	0.001552	3	36.6097	0.025043	2.45255	0.001619
4	47.8925	0.14161	1.89781	0.005265	4	47.897	0.187793	1.89764	0.006974
5	56.9474	0.104195	1.61567	0.002703	-	-	-	-	-
6	63.0833	0.127888	1.47248	0.002672	5	63.2454	0.102472	1.4691	0.00213

Firstly, it is obvious to see that these films maintain polycrystallinity. The three large signature peaks for the signature (100), (002), and (101) phases for ZnO are apparent. The 1% Ga:ZnO sample that was treated in a lower pressure of H_2 has peaks near 48°, 57°, and 63°, corresponding to the (102), (110), and (103) phases, respectively, with no secondary phases displayed. After an annealing treatment in twice the pressure of H_2 at 400°C for 1 hour, the (110) phase disappears. Just as we have seen in the 1% Al:ZnO, after multiple annealing treatments the film becomes more crystalline. Also, just like the 1% Al:ZnO, the low doping concentration and the hydrogen treatment do not cause a significant shift in the XRD peak positions.

Results for both 1% Al:ZnO and 1% Ga:ZnO show that hydrogen treatment does not seem to have a substantial effect on the crystal structure. The crystallinity of the thin film

increases due to multiple heat treatments. Neither the low concentrations of doping nor the annealing treatments appear to play a significant role in the XRD peak positions.

Although seemingly insignificant, it is clear to see that the optical and structural properties of doped and undoped zinc oxide thin films can be influenced by the addition of hydrogen into the lattice. As in many cases, it is also expected to see a significant change in the electrical properties of ZnO thin films.

3.4.3 Electrical properties: Hall Effect and van der Pauw methods

A preliminary measurement of the conductivity of undoped ZnO, 1% Al:ZnO, and 1% Ga:ZnO is made using a two-probe ohmeter on the surface of the ZnO thin films. The resistances of these thin films were measured during each step of the post synthesis treatment process.

Table 3.5 Two-probe surface resistance measurements for 1%Al:ZnO and 1%Ga:ZnO after various hydrogen treatment at 400°C. The table has "N/A" if the sample was not treated in the atmosphere specified by the column header. Samples were annealed in H_2 for 1 or 3 hours and at 2 and 5 times the amount of H_2 for 1 hour.

	H_2, 1hr	H_2, 3hr	2xH_2, 1hr	5xH_2, 1hr
1%Ga:ZnO AB	150-300 kΩ	150-300 kΩ	150-240 kΩ	N/A
1%Ga:ZnO BA	150-400 kΩ	150-400 kΩ	150-350 kΩ	N/A
1%Al:ZnO AB	150-250 kΩ	N/A	N/A	30-40kΩ

Preliminary measurements show that hydrogen also has a substantial effects on the electrical properties of the film, as the surface resistance greatly decreases when hydrogen is introduced to the material.

The length of anneal did not seem to have much if any effect on conductivity. Moreover, 5 times the pressure of the hydrogen showed an order of magnitude decrease in the surface resistance of these ZnO thin films, most likely due to more hydrogen compensating for zinc vacancies and creating hydrogen interstitials in the lattice. To further investigate the electrical properties, room temperature Hall Effect measurements of 1% Ga:ZnO on AB quartz treated in hydrogen are investigated.

The Hall Effect occurs when a current, *I*, is sent through the length, *l*, of a conductor in the x-direction, and an external magnetic field, *B*, is applied perpendicularly through the thickness, *t*, in the z-direction as seen in the following diagram.

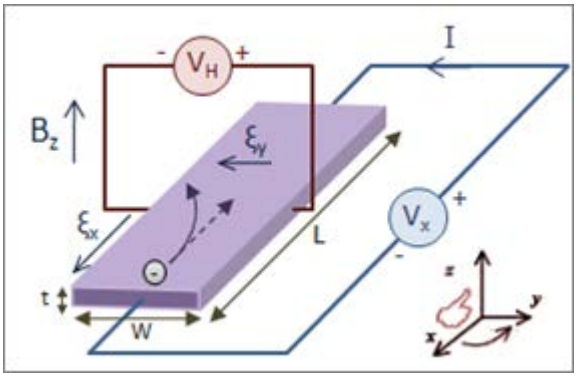

Figure 3.25 is the schematic of the Hall Effect to show that the charge carriers are forced to opposite walls when influenced by a B-Field [51].

In order to measure electrical properties using the Hall Effect, the van der Pauw method can be used to measure the sheet resistance. Using the van der Pauw method, 4 ohmic contacts can be applied to a semiconductor of flat shape and uniform thickness to measure resistivity, doping type, carrier concentration, and mobility. In general, van der Pauw's method cannot relate the sheet resistance in terms of known functions, except when the vertical and horizontal resistance *R* of the sample are equal.

Under this assumption, we can numerically solve for sheet resistance by the following equation:

$$R_s = \frac{\pi R}{\ln 2} \quad (1).$$

Thus, the resistivity, ρ, is then determined by multiplying R_s and t. When a magnetic field is present, these charge carriers experience a Lorentz Force:

$$F_1 = qvB \quad (2)$$

where q is the charge, v is the velocity and B is the magnetic field. This force deviates the charge carriers from the original "line of sight," causing electrons and holes to align themselves along opposite walls of the material, creating an electric field E with an equal and opposite force:

$$F_2 = Eq \quad (3).$$

where E equals the Hall voltage V_H divided by the width to give us the following relationship:

$$vB = \frac{V_H}{w} \quad (4)$$

where v of the charge carrier is I divided by the total charge, Q, which equals the product of the unit charge, e, the charge density, N, and the cross section, wt, of the semiconductor. By substituting these terms and rearranging, we solve for V_H:

$$\frac{IB}{eNt} = V_H \quad (5).$$

The Hall Voltage is measured and considering the directions of B and I, the polarity tells us the type of the material. If it is positive, it is p-type and if it is negative, it is n-type. Using this equation to solve for the magnitude of Nt, the sheet density can be determined. Dividing this numerical value by t, we know the majority carrier concentration, N. When the concentration of

one type is orders of magnitude larger than the other type, ρ can be used to solve for the mobility of the majority charge carriers, μ_m, as follows:

$$\mu_m = \frac{1}{eN\rho} \quad (6).$$

Table 3.6 The electrical properties of 14 layer 1%Ga:ZnO sample on AB Quartz annealed in various hydrogen treatments at 400°C measured by Hall and van der Pauw methods. The properties were measured at $I = 10 \times 10^{-6}$ A, $B = 4.86 \times 10^{-5}$ $\frac{V \cdot s}{cm^2}$ and $t = 454.16 \times 10^{-7}$ cm.

1%Ga:ZnO on AB quartz in Hydrogen	
Sheet Resistance (Ω/sq)	1.287×10^{5}
Resistivity (Ω·cm)	0.5845
Hall voltage (V), type	-2.66×10^{-6}
Carrier Concentration (cm^{-3})	2.514×10^{19}
Mobility ($cm^2/V \cdot s$)	0.0425

With this we know that 1% Ga:ZnO can be synthesized as a transparent n-type conductive oxide. Overall this film exhibited high transparency and UV absorbance, where treatment in hydrogen can substantially increase the overall conductivity. The film has a resistivity two orders of magnitude higher than found in [46] and [47] and has a carrier concentration on the same order. This increase in conductivity is due to hydrogen's n-type doping in ZnO. Hydrogen forms as interstitials which act as a donor and bring electrons to the conduction band or passivates deep acceptors that would be stealing electrons from the conduction band. Although, the 1% Ga:ZnO is not the best seen to date, it is definitely a transparent conductive oxide with promising tunability.

3.4.4 Conclusions

Optical and positron spectroscopy, XRD, and Hall Effect measurements tell us that the material properties are significantly affected by heat treatment in hydrogen atmospheres at 400ºC. When introducing hydrogen into doped and undoped zinc oxide thin films, the structure remains polycrystalline, but the defect concentration will decrease due to filled zinc vacancies. Hydrogen can also create a donor interstitial in these conditions. These processes will result in significant effects on the optical and electrical properties. As we do see a change in visible range absorbance because of a change in band gap defects, these zinc oxide thin films still essentially exhibit perfect transparency with high UV range absorbance. Furthermore, the electrical conductivity of these samples can be greatly enhanced using hydrogen annealing treatment to passivate deep acceptors in the material and act as a donor to increase the electrons in the conduction band. Using the sol-gel spin coating technique and annealing treatments in hydrogen, 1% Ga:ZnO thin film has also been synthesized as a high-quality TCO.

3.5 Zinc Annealing Treatment and Effects on Material Properties

Other donors, such as zinc interstitials, can be incorporated into the zinc oxide structure by similar heat treatment. Also, this zinc atmosphere can help passivate p-type zinc vacancies just as hydrogen does or create oxygen vacancies. A zinc atmosphere is created by wrapping a zinc oxide thin film in high purity zinc foil and annealing the sample in an inert nitrogen atmosphere at 400ºC. Zinc is deposited into the thin film structure and forms as interstitials and fills zinc vacancies, both of which lead to a structural change, affecting optical absorbance and electrical conductivity.

3.5.1 Optical Characterization

The following absorbance measurements will help us better understand the effects of a zinc atmosphere on the optical properties of zinc oxide thin films.

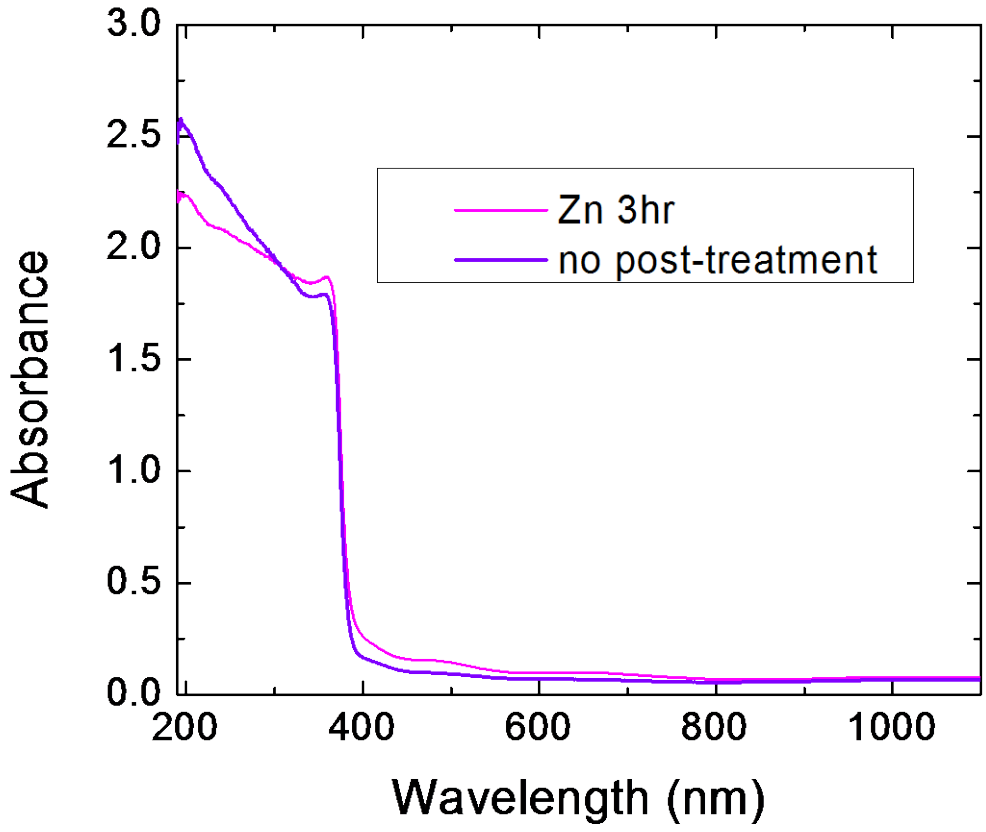

Figure 3.26 is the absorbance of undoped ZnO before and after annealing in Zn foil and N_2 atmosphere at 400ºC for 3 hours. These thin films all exhibit strong UV absorbance with a band gap near 380 nm. This time, the addition of zinc seems to have the opposite effect hydrogen has in the UV range, decreasing the slope of the absorbance per photon energy.

High transparency in the visible range for all samples is a good sign that band gap defects have been minimized and film quality improved.

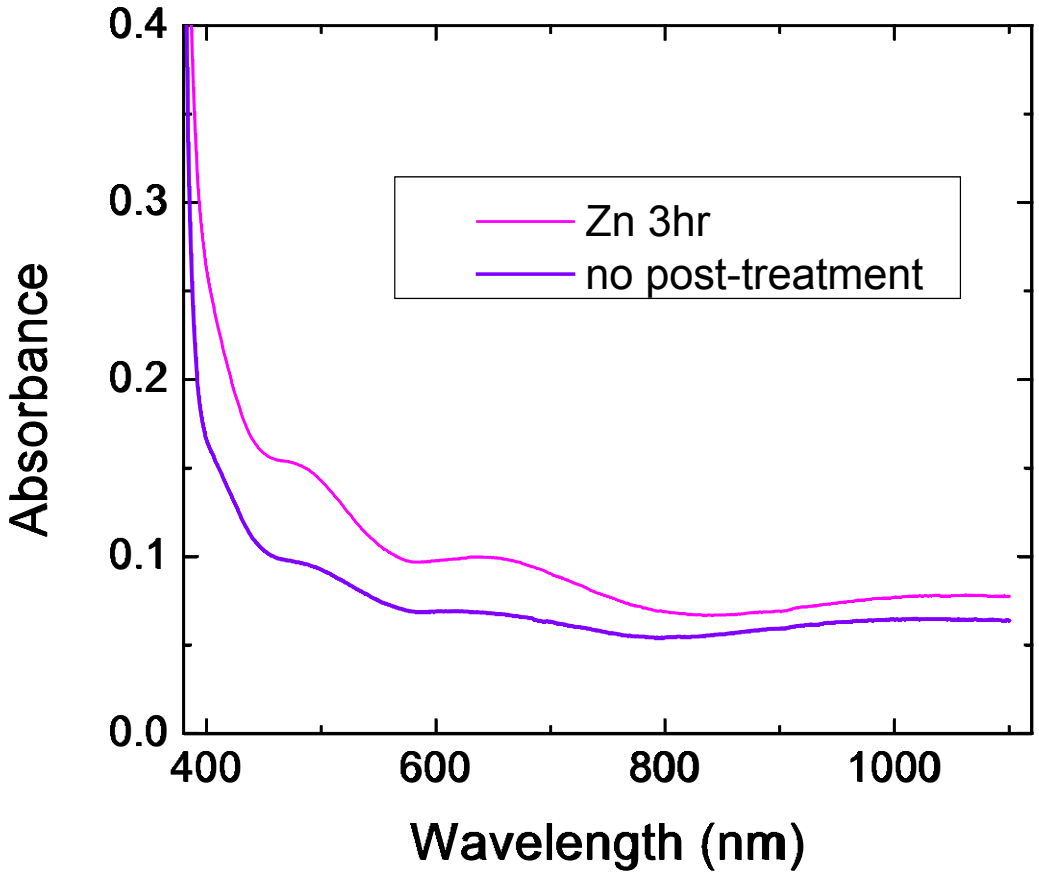

Figure 3.27 is the visible range absorbance of undoped ZnO before and after annealing in Zn foil and N_2 atmosphere at 400°C for 1 hour. ZnO thin films samples after annealing in a zinc atmosphere reveals a significant increase in visible range absorbance. Zinc treatment causes some oxygen vacancies to form, which will absorb more visible range light.

A similar 1% Al:ZnO film was annealed in an H_2 atmosphere at 400°C for 1 hour, before treatment in zinc.

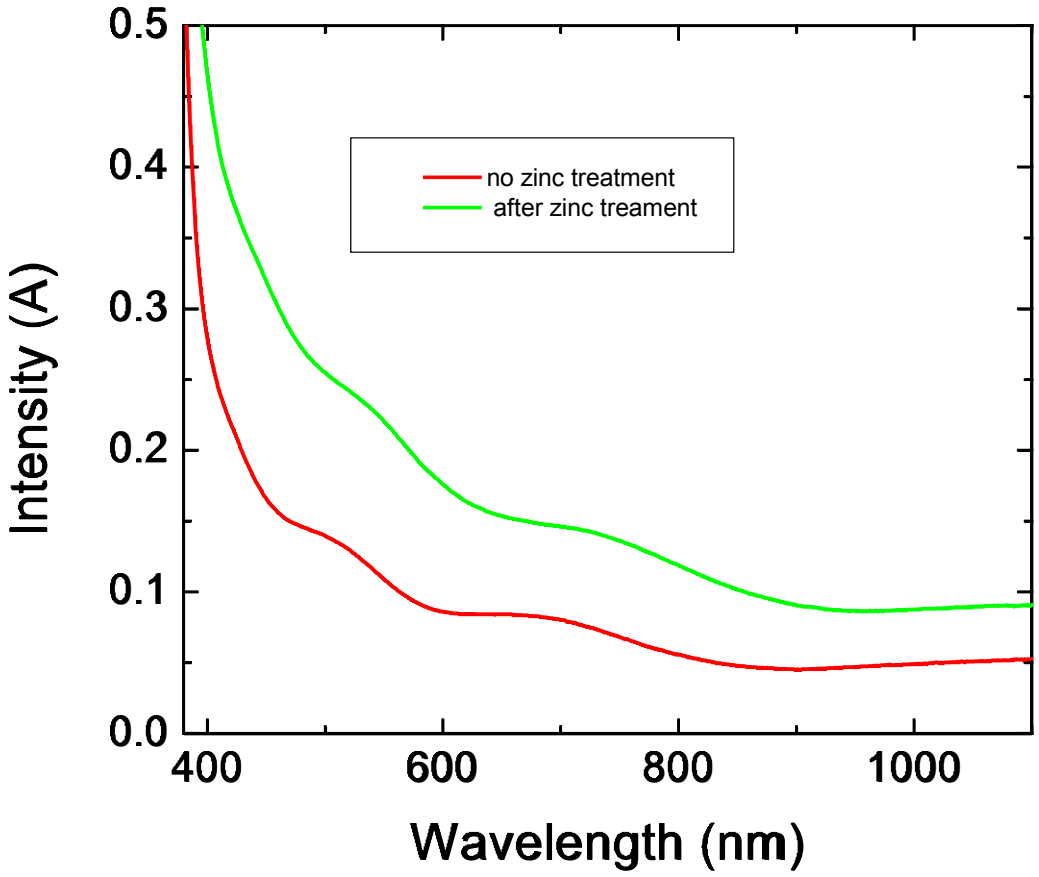

Figure 3.28 is the visible range absorbance of 1%Al:ZnO – annealed in air at 400°C for 1 hour, in H_2 at 400°C for 1 hour – before and after anneal in zinc foil in N_2 at 400°C for 1 hour. We see the same increase in absorbance due to zinc treatment creating more oxygen vacancies.

Therefore, this change occurs solely because of the addition of zinc into the material regardless of the hydrogen in the sample. The effects of zinc on the zinc oxide thin film structure are studies using XRD.

3.5.2 XRD Characterization

Undoped ZnO, 1% Al:ZnO and 1% Ga:ZnO thin films were synthesized using the sol-gel technique and annealed in various zinc atmospheres. Some thin films were annealed in hydrogen after synthesis and prior to zinc treatment. XRD measurements were used to see the effects of incorporating extra zinc into the lattice.

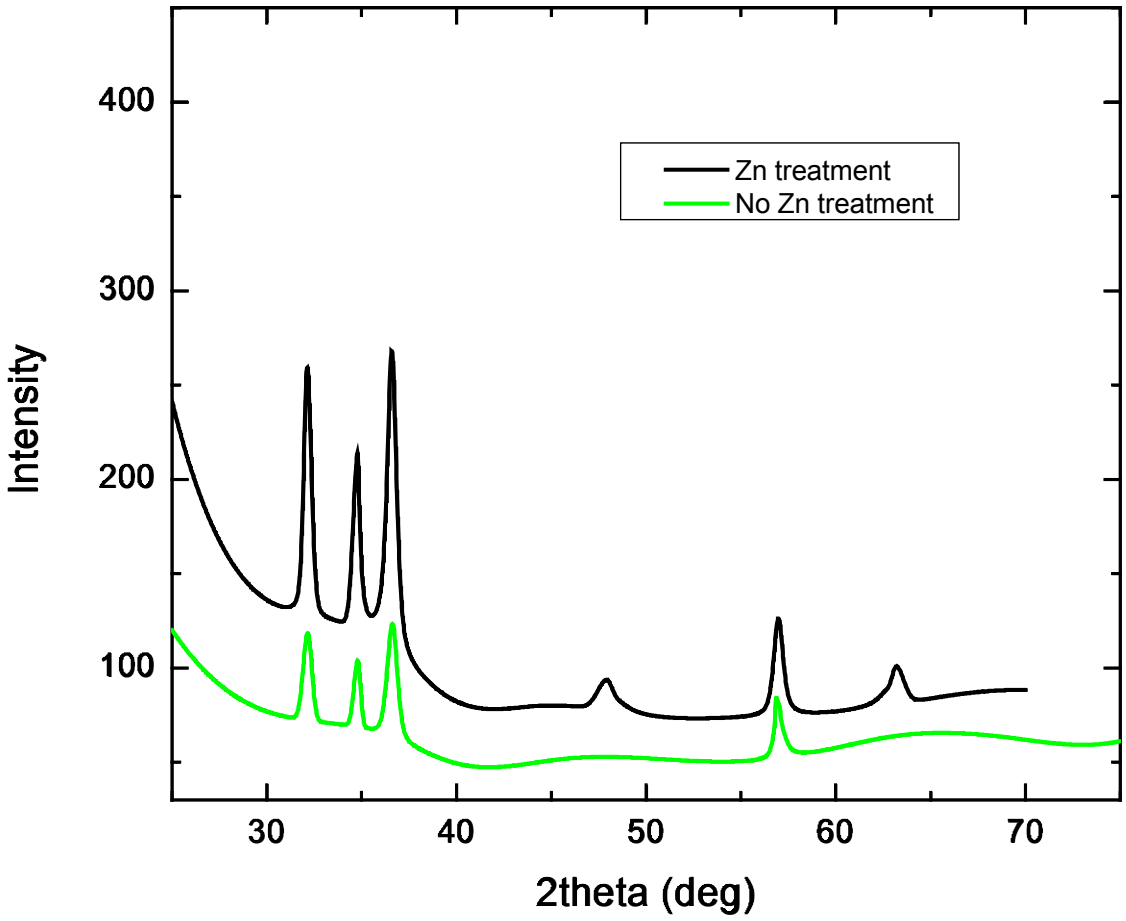

Figure 3.29 shows the XRD patterns for 12 layer Undoped ZnO on AB etched quartz before and after treatment in zinc atmosphere at 400°C for 3 hours. The crystal phases for ZnO and Al_2O_3 are in Appendices A and B.

Table 3.7 XRD peak positions, separation and phase for 12 layer Undoped ZnO on AB etched quartz before and after treatment in zinc atmosphere.

Undoped ZnO					Undoped ZnO, Zinc treatment				
Peak No.	2θ (deg)	ESD of 2θ	d(Å)	ESD of d	Peak No.	2θ (deg)	ESD of 2θ	d(Å)	ESD of d
1	32.1284	0.046488	2.78367	0.003916	1	32.0978	0.025243	2.78625	0.002132
2	34.7698	0.058412	2.578	0.00419	2	34.7789	0.019307	2.57735	0.001386
3	36.5966	0.045843	2.4534	0.002964	3	36.5557	0.028419	2.45606	0.001843
-	-	-	-	-	4	47.9135	0.081292	1.89702	0.003023
4	56.8583	0.040617	1.61799	0.001059	5	56.9316	0.078144	1.61608	0.00203
					6	63.0978	0.110731	1.47218	0.002313

Again, we see the signature (100), (002), (101), and (110) phases for ZnO thin film polycrystallinity. After annealing in a zinc atmosphere there is a strong increase in all phases peaks and a formation of the (102) and (103) peaks with insignificant shifts in *2θ*. This could be due to new layers of ZnO forming, increasing the number of ZnO phases. In order for this to happen, the zinc in the atmosphere would extract and bond with oxygen from the sample, depositing a new layer and creating more oxygen vacancies simultaneously. For comparison, 1% Al:ZnO films post-annealed in H_2 at 400ºC for 1 hour were treated in zinc.

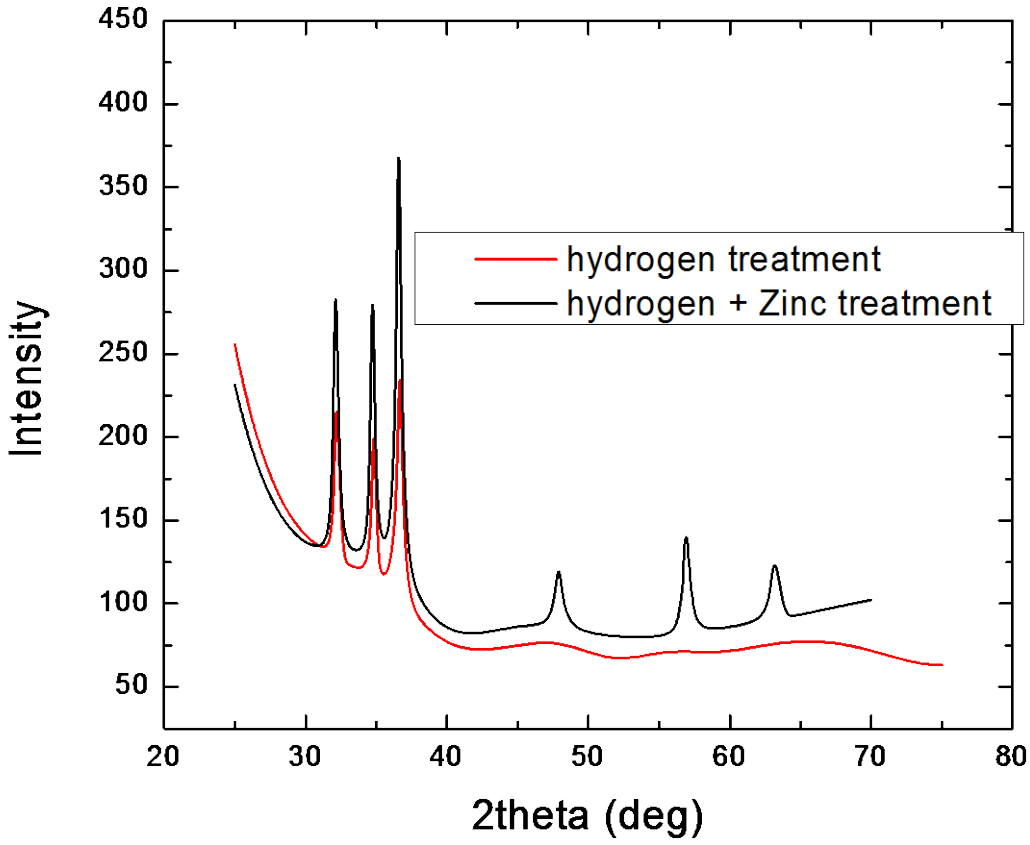

Figure 3.30 shows the XRD patterns for 16 layer 1% Al:ZnO on AB etched quartz – and post-annealed in H_2 at 400°C – before and after treatment in zinc atmosphere at 400°C for 1 and 3 hours. Crystal phases for ZnO and Al_2O_3 are in Appendices B and C.

Table 3.8 XRD peak positions, separation and phase for 16 layer 1% Al:ZnO on AB etched quartz –post-annealed in H_2 at 400ºC – before and after treatment in zinc atmosphere.

1% Al:ZnO (annealed in Hydrogen)					1% Al:ZnO (annealed in Hydrogen), Zinc treatment				
Peak No.	2θ (deg)	ESD of 2θ	d(Å)	ESD of d	Peak No.	2θ (deg)	ESD of 2θ	d(Å)	ESD of d
1	32.1095	0.022474	2.78527	0.001897	1	32.0878	0.027038	2.7871	0.002285
2	34.7975	0.046161	2.57602	0.003307	2	34.7078	0.033262	2.58247	0.002396
3	36.6578	0.037658	2.44944	0.002427	3	36.5587	0.015288	2.45586	0.000991
					4	47.8611	0.104371	1.89898	0.003889
					5	56.8203	0.040446	1.61898	0.001056
					6	63.06	0.075475	1.47297	0.001579

We see the (100), (002), and (101) phases for the Al:ZnO thin film both with and without zinc treatment. After annealing in a zinc atmosphere there is a strong increase in all phases peaks and a formation of the (102), (110), and (103) peaks. When treated in hydrogen, the increased crystallinity was attributed to length of annealing. This time, there is an increase in phases after zinc treatment, even when the thin film was annealed for 5 or more hours total. Again, more ZnO could be forming new layers and creating oxygen vacancies, leading to the formation of other phases. Regardless of the aluminum doping, we see this effect after annealing in a zinc atmosphere. For all undoped and Al-doped ZnO films studied by XRD there is a change structural properties. The Hall Effect will be used to measure the electrical properties.

3.5.3 Electrical Properties: Hall Effect and van der Pauw Methods

Various zinc oxide thin films were annealed in this zinc atmosphere, some after previously being annealed in hydrogen. After post annealing in zinc, all zinc oxide thin films showed a substantial decrease in two-probe resistance measurements.

Table 3.9 Two-probe surface resistance measurements for ZnO thin films after zinc treatment at 400°C. Some samples were previously treated in hydrogen atmospheres at 400°C. "N/A" is used if the sample was not treated in the atmosphere specified in the column header and "O.L" is used if the sample is too resistive to measure.

	400°C, H_2, 1hr	400°C, (4% H_2:96% N_2), 1hr	Wrap in Zn foil 400°C, N_2, 1 hr	Wrap in Zn foil 400°C, N_2, 3 hr
1--1%Ga:ZnO	150-300 kΩ	N/A	4-40 kΩ	N/A
2--1%Al:ZnO	150-400 kΩ	N/A	4-8 kΩ	0.7-1.1 kΩ
3--Undoped ZnO	O.L	O.L	N/A	1.0-1.7 MΩ
4--Undoped ZnO	O.L	N/A	N/A	3.1-25 MΩ

Through these results, we see that the addition of zinc will in fact increase the conductivity in all undoped, Ga-doped, and Al-doped ZnO thin films. To measure the electrical properties, room temperature Hall Effect was measured and results are summarized in the following table.

Table 3.10 The electrical properties of doped and undoped ZnO thin films after final treatment in zinc atmosphere at 400°C measured by Hall and van der Pauw methods. *I*, *B* and *t* are also listed first and used in their respective calculations.

	1--14 layer 1%Ga:ZnO	2--16 layer 1%Al:ZnO	3--10 layer Undoped ZnO	4--12 layer Undoped ZnO
B- field ($V \cdot s/cm^2$)	4.86×10^{-5}	4.86×10^{-5}	4.86×10^{-5}	4.86×10^{-5}
Current (A)	100×10^{-6}	100×10^{-6}	100×10^{-9}	100×10^{-9}
Thickness (cm)	454.16×10^{-7}	519.04×10^{-7}	324.4×10^{-7}	389.28×10^{-7}
Sheet Resistance (Ω/sq)	2438	331.5	3052	6.269×10^{6}
Resistivity (Ω·cm)	0.1107	0.0172	0.099	244.04
Hall voltage (V)	2.62×10^{-6}	1.95×10^{-7}	4.36×10^{-7}	9.45×10^{-6}
Carrier Concentration (cm^{-3})	2.553×10^{20}	3.001×10^{21}	2.14×10^{18}	8.257×10^{16}
Mobility ($cm^2/V \cdot s$)	0.221	0.121	29.4	0.31

Incorporating zinc can have a significant increase the overall conductivity. Every time a doped or undoped ZnO film was annealed in a zinc atmosphere, there was a large decrease in sheet resistance. This could be due to the addition of n-type zinc interstitials introduced into the lattice or zinc vacancies being filled, compensating some acceptors in the material. Also, a new layer of ZnO could be forming to help increase overall n-type conductivity. Two of the films in this table have a carrier concentration at least one order of magnitude higher than the reports in [45]. 1% Ga:ZnO annealed in H_2 and then zinc has an exceptional carrier concentration of 2.553

$\times 10^{20}$ electrons/cm^3. 1% Al:ZnO was also annealed in H_2 first then underwent two annealing procedures in zinc, lasting a total of three hours more than the 1% Al:ZnO treatment. This Al:ZnO thin film has a higher carrier concentration of 3.001×10^{21} electrons/cm^3.

3.5.4 Conclusions

Characterization of these ZnO thin films helps us understand the effects of treatment in a zinc-rich environment at 400ºC. Introducing more zinc into doped and undoped zinc oxide thin films increases the n-type conductivity by passivating acceptor zinc vacancies and adding donors by creating zinc interstitials. This causes an increase in oxygen vacancies, and thus, the visible range absorbance. Still, these zinc oxide thin films essentially exhibit perfect transparency with high UV range absorbance. Therefore, it is obvious to see that the incorporation of zinc treatment allows for successful synthesis of ZnO thin films as a TCO by way of the sol-gel spin coating method.

3.6 References

[48] "Scanning Electron Microscope." *Academic Dictionaries and Encyclopedias*. N.p., n.d. Web. 10 June 2015. <http://en.academic.ru/dic.nsf/enwiki/17217>.

[49] "TP1: Colorantes Orgánicos." *Colorantes Orgánicos*. N.p., n.d. Web. 10 June 2015. <http://www2.fisica.unlp.edu.ar/materias/experimentoscuanticosI/TP_Cianinas/PerkinElmer_Lambda25_manual.pdf>.

[50] "Quantum Dot." *Wikipedia*. Wikimedia Foundation, n.d. Web. 10 June 2015. <http://en.wikipedia.org/wiki/Quantum_dot>.

[51] "Hall Effect." *Wikipedia*. Wikimedia Foundation, n.d. Web. 10 June 2015. <http://en.wikipedia.org/wiki/Hall_effect>.

CHAPTER 4: CONCLUSIONS AND FUTURE WORK

It is apparent that the electrical properties of zinc oxide thin films can be significantly affected by the addition of hydrogen and zinc into the material. These atmospheres are used to compromise passivate acceptors and create donor like interstitials within the lattice. Furthermore aluminum seems to be a better dopant than gallium in order to achieve higher conductivity, but the doping agents and percentages must be investigated further to fully understand the effects. All-in-all, high quality transparent conductive zinc oxide thin films can be synthesized by our revised sol-gel spin coating technique and the electrical properties can be greatly enhanced by treatment in hydrogen and zinc atmospheres.

To successfully synthesize highly transparent uniform undoped, Al-, and Ga-doped zinc oxide thin films solutions must be monitored to maintain consistent viscosity, substrates must be etched in piranha AB to create a compatible interface, the layering must be controlled by a manual syringe, and the temperature stabilized to maintain consistency and uniformity. After successfully synthesizing uniform transparent zinc oxide thin films, the overall electrical conductivity can be substantially increased by the incorporation of zinc and hydrogen through simple heat treating procedures. Heat treatment in hydrogen uses electrically active H^+ to passivate lattice defects to compensate fill acceptor vacancies and create hydrogen interstitials to add donors and improve the overall conductivity. In addition, heat treatment with the incorporation of zinc allows zinc ions to deposit into the ZnO lattice, filling zinc vacancies and creating zinc interstitials, both of which can help increase the electrical conductivity.

There are many variables to account for during the sol-gel spin coating method, all of which can greatly affect the structural, optical, and electrical properties of doped and undoped

zinc oxide. Future work must be done in each step of this process to fully understand the effects on thin film quality.

Firstly, the doping of the precursor solution can be optimized with different amounts of group III metals like aluminum and gallium to add donors and enhance n-type conductivity, without compromising transparency and structure. The spin coating and drying techniques can be improved to affect film quality and save time. To reduce environmental impurities, the sol-gel spin coating should take place in a clean room. Also, changing the acceleration rates will yield different thicknesses and can affect substrate coverage. Spin coating thin films while the solution is at a higher viscosity could improve consistency and lead to more precise layering as the solution can move more easily amongst itself. The drying temperature can be varied or a different type of irradiation can be used to evaporate solvent and yield different structures, possibly affecting the conductivity. Although transparent conductive zinc oxide is successfully synthesized using our technique, redevelopment to better control this process should increase overall film quality, providing better insight on the material properties.

Post-synthesis treatments are also subject to further investigation. This work shows an increase in sheet resistance after annealing ZnO thin films in hydrogen and zinc, separately. The addition of hydrogen and zinc both increase the n-type conductivity by passivating acceptor vacancies and adding donors to the material. Furthermore, treating these samples in a series of hydrogen and zinc will lead to n-type carrier concentrations as high as 3.001×10^{21} cm^{-3}. Although hydrogen can increase conductivity, zinc have a more substantial effect. The pressures and temperatures of these atmospheres can be modified to tune electrical properties.

Current, preliminary measurements show 16 layer 2% Al:ZnO thin films exhibit high visible range transparency and increased conductivity after treatment in hydrogen and zinc

atmospheres. The resistance of 3-10 kΩ is slightly less than the resistance of 1% Al:ZnO from this thesis, leading us to believe 1% is a better doping percentage.

Hall Effect measurements will determine which doping percentage of aluminum will have better conductivity. Full characterization must also be done to determine the doping effects on the material properties.

APPENDIX A: DOPED AND UNDOPED ZnO THIN FILMS SYNTHESIZED BY SOL-GEL SPIN COATING

Substrate	Substrate Etch	Doping agent	Doping %	# of Layers	Comments
11.3mmx13.9mm fused silica	-	-	-	6	Lack of coverage
12.4mmx11.2mm fused silica	-	$Cu(CH_3COO)_2 \cdot 2H_2O$	1.0%	6	Lack of coverage
10mmx10mm sapphire	-	$Cu(CH_3COO)_2 \cdot 2H_2O$	1.0%	6	Lack of coverage
10mmx10mm sapphire	-	$Na(CH_3COO)$	1.0%	6	Lack of coverage
10mmx10mm sapphire	-	$In(CH_3COO)_2 \cdot xH_2O$	1.0%	6	Lack of coverage
10mmx10mm sapphire	-	$GaCl_3$	1.0%	6	Lack of coverage
1in diameter quartz	AB	$Al(CH_3COO) \cdot OH$	3.0%	6	Some good Coverage
1in diameter quartz	BA	$Al(CH_3COO) \cdot OH$	3.0%	6	Some good Coverage
1in diameter quartz	AB	$AlCl_3$	3.0%	6	Some Coverage
1in diameter quartz	BA	$AlCl_3$	3.0%	6	Lack of coverage
1in diameter quartz	AB	$Al(CH_3COO) \cdot OH$	3.0%	12	Inconsistent coverage
1in diameter quartz	BA	$Al(CH_3COO) \cdot OH$	3.0%	12	Inconsistent coverage
1in diameter quartz	AB	$AlCl_3$	3.0%	12	Full good coverage
1in diameter quartz	BA	$AlCl_3$	3.0%	12	Full good coverage
~10mmx10mm fused silica	-	$AlCl_3$	3.0%	12	Inconsistent coverage
~10mmx10mm fused silica	-	$AlCl_3$	3.0%	12	Inconsistent coverage
10mmx10mm sapphire	-	$AlCl_3$	3.0%	10	Inconsistent coverage
10mmx10mm sapphire	-	$AlCl_3$	3.0%	12	Inconsistent coverage
~10mmx10mm fused silica	AB	$AlCl_3$	3.0%	12	Inconsistent coverage
~10mmx10mm fused silica	BA	$AlCl_3$	3.0%	12	Inconsistent coverage

10mmx10mm sapphire	AB	$AlCl_3$	3.0%	12	Inconsistent coverage
10mmx10mm sapphire	BA	$AlCl_3$	3.0%	12	Inconsistent coverage
~10mmx10mm fused silica	AB	$AlCl_3$	3.0%	24	Inconsistent coverage
~10mmx10mm fused silica	BA	$AlCl_3$	3.0%	24	Inconsistent coverage
10mmx10mm sapphire	AB	$AlCl_3$	3.0%	24	Inconsistent coverage
10mmx10mm sapphire	BA	$AlCl_3$	3.0%	24	Inconsistent coverage
10mmx10mm sapphire	AB	$AlCl_3$	4.0%	24	Inconsistent coverage
25mmx25mm quartz	AB	$AlCl_3$	3.0%	12	Inconsistent coverage
25mmx25mm quartz	BA	$AlCl_3$	3.0%	12	Inconsistent coverage
25mmx25mm quartz	AB	$AlCl_3$	1.0%	12	Inconsistent coverage
25mmx25mm quartz	BA	$AlCl_3$	1.0%	12	Inconsistent coverage
25mmx25mm quartz	AB	-	-	24	Inconsistent coverage
1in diameter quartz	BA	$AlCl_3$	1.0%	24	Inconsistent coverage
1in diameter quartz	AB	$AlCl_3$	2.0%	24	Inconsistent coverage
1in diameter quartz	BA	$AlCl_3$	3.0%	24	Inconsistent coverage
1in diameter quartz	AB	$Al(CH_3COO)\cdot OH$	1.0%	16	Inconsistent coverage
1in diameter quartz	BA	$Al(CH_3COO)\cdot OH$	1.0%	16	Inconsistent coverage
1in diameter quartz	AB	$Al(NO_3)_3\cdot 9H_2O$	1.0%	16	Full consistent coverage
1in diameter quartz	BA	$Al(NO_3)_3\cdot 9H_2O$	1.0%	16	Full consistent coverage
1in diameter quartz	AB	$Al(NO_3)_3\cdot 9H_2O$ **	1.0%	24	Full consistent coverage
1in diameter quartz	AB	$AlCl_3$ **	1.0%	24	Inconsistent coverage

1in diameter quartz	AB	$Al(NO_3)_3 \cdot 9H_2O$	1.0%	16	Full consistent coverage
1in diameter quartz	AB	$Al(NO_3)_3 \cdot 9H_2O$	1.0%	16	Full consistent coverage
1in diameter quartz	AB	$Al(NO_3)_3 \cdot 9H_2O$	2.0%	16	Full consistent coverage
1in diameter quartz	BA	$Al(NO_3)_3 \cdot 9H_2O$	3.0%	16	Full consistent coverage
1in diameter quartz	AB	$Al(NO_3)_3 \cdot 9H_2O$	0.5%	16	Full consistent coverage
1in diameter quartz	AB	$Al(NO_3)_3 \cdot 9H_2O$	0.5%	16	Full consistent coverage
1in diameter quartz	-	$Al(NO_3)_3 \cdot 9H_2O$	1.00%	12	Full consistent coverage
1in diameter quartz	IPA Ultrasonic	Al(CH3COO)·OH	2.0%	15	Inconsistent coverage
		Co(CH3COO)2·4H2O	3.0%		Inconsistent coverage
1in diameter quartz	IPA Ultrasonic	Co(CH3COO)2·4H2O	3.0%	15	Inconsistent coverage
					Inconsistent coverage
1in diameter quartz	AB	$Al(NO_3)_3 \cdot 9H_2O$	2.0%	16	Cloudy green film
		Co(CH3COO)2·4H2O	3.0%		Cloudy green film
1in diameter quartz	AB	Mn(CH3COO)2·4H2O	3.0%	16	Inconsistent coverage
1in diameter quartz	AB	$Al(NO_3)_3 \cdot 9H_2O$	1.0%	16	consistent coverage
1in diameter quartz	AB	$Al(NO_3)_3 \cdot 9H_2O$	1.0%	16	consistent coverage
1in diameter quartz	AB	-	-	12	consistent coverage
1in diameter quartz	AB	-	-	12	consistent coverage
1in diameter quartz	BA	$Al(NO_3)_3 \cdot 9H_2O$	1.0%	16	consistent coverage

1in diameter Sapphire	AB	$Al(NO_3)_3 \cdot 9H_2O$	1.0%	16	consistent coverage
1in diameter quartz	AB	$Ga(NO_3)_3 \cdot xH_2O$	1.0%	14	consistent coverage
1in diameter quartz	BA	$Ga(NO_3)_3 \cdot xH_2O$	1.0%	16	consistent coverage
1in diameter quartz	AB	$Ga(NO_3)_3 \cdot xH_2O$	1.5%	16	consistent coverage
1in diameter quartz	BA	$Ga(NO_3)_3 \cdot xH_2O$	1.5%	16	consistent coverage
1in diameter quartz	AB	$Ga(NO_3)_3 \cdot xH_2O$	1.0%	16	consistent coverage
1in diameter quartz	AB	$Al(NO_3)_3 \cdot 9H_2O$	1.0%	16	consistent coverage

APPENDIX B: STANDARD X-RAY PATTERS FOR ZnO

2θ (º)	d (nm)	(h k l)
31.802	0.28116	(1 0 0)
34.447	0.26015	(0 0 2)
36.289	0.24735	(1 0 1)
47.583	0.19095	(1 0 2)
56.659	0.16233	(1 1 0)
62.913	0.14761	(1 0 3)
66.453	0.14058	(2 0 0)
68.02	0.13772	(1 1 2)
69.166	0.13571	(2 0 1)
72.626	0.13008	(0 0 4)
77.047	0.12368	(2 0 2)
81.461	0.11805	(1 0 4)
89.715	0.10921	(2 0 3)
92.916	0.10412	(2 1 0)
95.435	0.10412	(2 1 1)
98.729	0.10151	(1 1 4)
103.075	0.09838	(2 1 2)
104.243	0.09759	(1 0 5)
107.571	0.09547	(2 0 4)
110.556	0.09372	(3 0 0)
116.449	0.09061	(2 1 3)
121.767	0.08817	(3 0 2)
125.318	0.08672	(0 0 6)
134.14	0.08364	(2 0 5)
136.739	0.08286	(1 0 6)
138.786	0.08229	(2 1 4)
143.273	0.08116	(2 2 0)

[54] "Introduction to ICSD Web." *ICSD*. N.p., n.d. Web. 10 June 2015. <https://icsd.fiz-karlsruhe.de/search/index.xhtml;jsessionid=AA885BB9EF47A9D2C58816C9603C1F0C>.

APPENDIX C: STANDARD X-RAY PATTERNS FOR Al_2O_3

2θ (º)	d (nm)	(h k l)
25.682	0.34659	(0 1 2)
35.307	0.25401	(1 0 4)
37.928	0.23703	(1 1 0)
41.878	0.21554	(0 0 6)
43.538	0.2077	(1 1 3)
46.371	0.19565	(2 0 2)
52.782	0.1733	(0 2 4)
57.768	0.15947	(1 1 6)
59.996	0.15407	(2 1 1)
61.395	0.15089	(1 2 2)
61.608	0.15042	(0 1 8)
66.82	0.1399	(2 1 4)
68.51	0.13685	(3 0 0)
70.745	0.13306	(1 2 5)
74.676	0.127	(2 0 8)
77.287	0.12335	(1 0 10)
77.64	0.12288	(1 1 9)
80.824	0.11882	(2 1 7)
81.077	0.11852	(2 2 0)
83.632	0.11553	(0 3 6)
84.764	0.11428	(2 2 3)
85.548	0.11343	(1 3 1)
86.771	0.11214	(3 1 2)
86.959	0.11195	(1 2 8)
89.493	0.10942	(0 2 10)
91.245	0.10777	(0 0 12)
91.651	0.1074	(1 3 4)
95.318	0.10421	(3 1 5)
95.757	0.10385	(2 2 6)
98.911	0.10137	(0 4 2)
101.676	0.09935	(2 1 10)
103.471	0.09811	(1 1 12)
103.889	0.09783	(4 0 4)
105.246	0.09693	(1 3 7)
110.171	0.09394	(3 2 1)
110.572	0.09371	(1 2 11)

111.678	0.09309	(3 1 8)
114.81	0.09143	(2 2 9)
116.825	0.09043	(3 2 4)
117.458	0.09012	(0 1 14)
118.591	0.08959	(4 1 0)
121.005	0.0885	(2 3 5)
122.848	0.08771	(1 4 3)
125.494	0.08665	(0 4 8)
128.669	0.08546	(1 3 10)
130.949	0.08467	(0 3 12)
132.246	0.08424	(2 0 14)
133.268	0.08391	(3 2 7)
133.785	0.08375	(2 1 13)
137.221	0.08273	(1 4 6)
140.699	0.08179	(3 1 11)
142.051	0.08146	(5 0 2)
142.357	0.08138	(2 3 8)
143.869	0.08102	(1 1 15)
146.725	0.0804	(4 0 10)

[54] "Introduction to ICSD Web." *ICSD*. N.p., n.d. Web. 10 June 2015. <https://icsd.fiz-karlsruhe.de/search/index.xhtml;jsessionid=AA885BB9EF47A9D2C58816C9603C1F0C>.